Temporal alterations to central auditory processing without synaptopathy after lifetime exposure to environmental noise

Florian Occelli, Florian Hasselmann, Jérôme Bourien, Jean-Luc Puel, Nathalie Desvignes, Bernadette Wiszniowski, Jean-Marc Edeline, Boris Gourévitch

Temporal alterations to central auditory processing without synaptopathy after lifetime exposure to environmental noise

Florian Occelli[1,a], Florian Hasselmann[2], Jérôme Bourien[2], Jean-Luc Puel[2], Nathalie Desvignes[1], Bernadette Wiszniowski[1], Jean-Marc Edeline[1,5], Boris Gourévitch[1,3,4,5]

[1]NeuroScience Paris-Saclay Institute (NeuroPSI), CNRS, University of Paris-Saclay, F-91405 Orsay, France

[2]Institute for Neurosciences of Montpellier (INM), INSERM, University of Montpellier, F-34091 Montpellier, France.

[3]Institut de l'Audition, Institut Pasteur, INSERM, F-75012 Paris, France.

[4]CNRS, France.

[5]These authors contributed equally

a: now at International Research Center for NeuroIntelligence (IRCN), University of Tokyo, Japan

Address correspondence to:

Boris Gourévitch

Institut de l'Audition,

63 rue de Charenton,

75012 Paris, France.

E-mail: boris@pi314.net

Phone: (+33) 1 76 53 50 41

Abbreviations

ABRs: auditory brainstem recordings

BF: best frequency

CAPs: compound action potentials

DPOAEs : distortion product otoacoustic emissions

ESR: evoked-to-spontaneous firing rate ratio

FR: firing rate

IHC: inner hair cell

PSTHs: post-stimulus time histograms

RDS: random double sweep

SNR: signal-to-noise ratio

STRF: spectrotemporal receptive field

TMTF: temporal modulation transfer function

TTS: temporary threshold shift

VS: vector strength

Keywords: auditory cortex, auditory brainstem response, compound action potential, synaptic ribbons, behavioral task, passive noise exposure.

Abstract

People are increasingly exposed to environmental noise, through the cumulation of occupational and recreational activities, which is considered harmless to the auditory system if the sound intensity remains <80 dB. However, recent evidence of noise-induced peripheral synaptic damage and central reorganizations in the auditory cortex, despite normal audiometry results, have cast doubt on the innocuousness of lifetime exposure to environmental noise. We addressed this issue, by exposing adult rats to realistic and non-traumatic environmental noise, within the daily permissible noise exposure limit for humans (80 dB SPL, 8 hours per day) for between 3 and 18 months. We found that temporary hearing loss could be detected after six months of daily exposure, without leading to permanent hearing loss or to missing synaptic ribbons in cochlear hair cells. The degraded temporal representation of sounds in the auditory cortex after 18 months of exposure was very different from the effects observed after only three months of exposure, suggesting that modifications to the neural code continue throughout a lifetime of exposure to noise.

Introduction

In recent decades, people have been exposed to increasing environmental noise, defined as the sum of noise from transport, professional and recreational activities. The cumulative effect of daily exposure to environmental noise, at loud but non-traumatic sound pressure levels, such as 80 dB SPL (sound pressure level), has long been considered harmless to the auditory system, even at the scale of a lifetime of exposure (ISO 1990).

This view is based principally on the absence of auditory threshold shifts after prolonged exposure to such levels of noise in humans (SCENIHR 2008; Prendergast et al. 2017) and animals

(Canlon and Fransson 1995; Willott and Bross 2004; Noreña et al. 2006). However, normal auditory thresholds do not fully reflect the health status of the peripheral auditory system: auditory thresholds can recover from a temporary threshold shift (TTS), experienced in the hours immediately following transient noise trauma. In rodents, a TTS is typically induced by exposing animals for a few hours to 100 dB SPL, and is accompanied by a loss of synaptic ribbons in the sensory inner hair cells, a decrease in the synchronized activity of the auditory nerve and subsequent degenerations of auditory nerve fibers (Kujawa and Liberman 2009) with no change in hearing thresholds, resulting in a "synaptopathy". If hearing damage were proportional to the acoustic energy received by the ear (Eldred et al. 1957), cumulative lifetime exposure to 80 dB SPL, which largely exceeds the energy delivered by synaptopathy-related protocols (100 dB SPL for 2 hours), should induce a TTS leading to long-term synaptopathy and, possibly, aggravated auditory aging.

Moreover, overstimulation with noise elicits auditory cortex plasticity. In adult animals, passive exposure, for one to three months, to noise levels <85 dB SPL with spectral or temporal narrowband acoustic content has been shown to modify the organization of the cortical circuits and to reduce the response to this specific content (Noreña et al. 2006; Zhou and Merzenich 2012). This reorganization may be governed by homeostatic plasticity (Gourévitch et al. 2014) and is partially reversible over a few weeks (Pienkowski and Eggermont 2012). Long-term noise exposure may also favor subsequent plastic changes, as if a new critical window had been opened in adulthood (Zhou et al. 2011; Thomas, Friedman, et al. 2019; Thomas et al. 2020), but could also lead to auditory disorders, such as hyperacusis (Thomas, Guercio, et al. 2019). However, it remains unclear how perception of auditory stimuli is altered by all these plastic changes.

All the animal studies described above used relatively short periods of exposure, at the scale of rodent life, and unrealistic types of environmental noise, such as broadband noise, noise bursts or random pure tones. The potential of a lifetime of exposure to realistic environmental noise to induce a TTS, to alter the neural representation of sounds, to impair behavioral performance, or to exacerbate the auditory aging process is an issue of the utmost concern in auditory neuroscience, but is currently unknown.

We evaluated the impact on the auditory system of adult rats of long-term (3 months) to lifetime (18 months) exposure to realistic non-traumatic noise (80 dB SPL, 8 h/day). Unlike many previous studies, we assessed the consequences of such exposure for the cochlea, auditory nerve, brainstem, cortical response to various acoustic features and behavior in each animal. Contrary to the prevailing view, exposure to noise at this moderate intensity (80 dB SPL) led to a TTS occurring after six months, which was not accompanied by a classical pattern of synaptopathy. We also found that three months of exposure led to degradation of the evoked-to-spontaneous firing rate ratio in the auditory cortex, whereas a lifetime of noise exposure led, instead, to degradation of the temporal representation of sounds. These findings suggest that repeated daily noise exposure, at a moderate SPL, may alter progressively the auditory system function over a period of years.

Methods

With the exception of noise exposure, the methods were as described in a previous study (Occelli et al. 2019) for which the control dataset was studied for specific aging effects. We therefore describe here only the most important points.

Subjects

Recordings were obtained from the primary auditory cortex of adult female Sprague Dawley rats. The animals were obtained from Janvier Laboratories at the age of two months, adapted for one month to the core animal facility, and housed for 3, 6, 12, or 18 months (the groups are named according to these time periods) in either a classical facility (unexposed animals) or a dedicated facility (exposed animals) with controlled humidity (50-55%) and temperature (22-24 °C) conditions, under a 12 h light/12 h dark cycle (lights on at 7:30 a.m.) with free access to food and water. At the end of experiments, animals were 6, 9, 15, or 21 months old. The initial number of animals was 10 for the 3-, 6-, and 12-month groups, and 20 for the 18-month group. We chose female rats, as they typically show less aggressive behaviors than males in groups of a few animals (Schweinfurth 2020) and are as good as, if not better than, male rats in shock avoidance tasks (Dalla and Shors 2009). Given the well-documented susceptibility of female Sprague Dawley rats to mammary tumors (Davis et al. 1956; Freedman et al. 1990; Fay et al. 1997; Jowa and Howd 2011), all aged animals were examined three times/week by staff from the animal facility, and any animal with tumors was excluded from the study. The final sample sizes for the various groups of animals are summarized in Supplementary Table 1. The protocol was approved by the local ethics committee (Paris-Sud University, CEEA No. 59, project 2014-25). Each animal was subjected to the sequence of protocols displayed in Fig. 1b and detailed below.

Environmental noise exposure

The dedicated facility had thick walls and was specially built for the project. Four cages, each housing three to four animals, were placed 1.5 m away (Supp. Fig. 1d) from a full-range powerful speaker (Adam A8X). Environmental noise exposure for 20 minutes was generated at

a sampling rate of 96 kHz from a Dynamic Moving Ripple (Kowalski et al. 1996; Escabi and Schreiner 2002) ranging between 100 and 40000 Hz with an instantaneous ripple density of 3 peaks/oct and an instantaneous modulation rate of 50 Hz. The stimulus was then amplitude-modulated by a temporal envelope obtained by low-pass filtering (Butterworth, frequency cutoff 5 Hz) a uniform white noise. The stimulus was rendered acoustically flat, by recording the speaker output within a cage (preamplifier 2169, transducer 4133, Bruel&Kjaer, Marantz PMD671 digital recorder), then inverting it and fitting a sixth-order IIR filter under Matlab (Matworks), which was then applied to the acoustic stimulus. The SPL was then adjusted to obtain 80±1 dB SPL in the four cages (Supp. Fig. 1d), with a Bruel&Kjaer 2250 soundmeter. The animals were exposed to the noise from 6 pm to 2 am each day, while they were in a waking state (at least most of the time), under the control of the task manager of Windows (Microsoft).

Auditory brainstem recordings

At several times during exposure for the 18-month group, and three weeks after the end of exposure, or at an equivalent age for control groups, auditory brainstem responses (ABRs) were obtained under isoflurane anesthesia (2.5%), by differential recordings between two subdermal electrodes (SC25, NeuroService) placed at the vertex and behind the mastoid bone. RTLab software (Echodia) was used to average 500 responses during the presentation of nine pure-tone frequencies (between 0.5 and 32 kHz) delivered by a speaker (Knowles Electronics) placed in the right ear of the animal. For each frequency, the threshold was determined by gradually decreasing the sound intensity (from 80 dB down to −10 dB SPL). The ABR threshold was defined as the minimum sound intensity eliciting a well-defined and reproducible wave II from the cochlear nucleus (Chen and Chen 1991).

157

158 Behavioral task

159 Rats were trained to discriminate between an amplitude-modulated white noise (4 Hz,
160 100% depth modulation; conditioned stimulus, CS+) and an unmodulated white noise (CS-) in
161 a two-compartment shuttle box. Both stimuli lasted 5 s, and they were presented a mean of 30
162 s apart (range: 20 s -75 s). The rat was required to change compartment on CS+ presentation.
163 A lack of response to the CS+ stimulus triggered a 0.3 mA footshock lasting for 10 s, which was
164 stopped immediately if the rat switched compartment. On presentation of the CS- signal, no
165 change in compartment was required. The CS+ and CS- stimuli were each presented 40 times
166 per session.

167 Performance was estimated by calculating the A' index (Verde et al. 2006), which is a
168 non-parametric analog of *d'* quantifying the discrimination between two stimuli, as follows:

169

170 $$A' = 12 + (H - F)(1 + H - F)4H(1 - F) \text{ if } H \geq F$$

171 and

172 $$A' = \frac{1}{2} + \frac{(F-H)(1+F-H)}{4F(1-H)} \text{ if } H<F$$

173 where *H* is the hit rate (the proportion of switches on CS+ presentation) and *F* is the false alarm
174 rate (the proportion of switches on CS- presentation). In our experiment, a successful session
175 was defined as a session in which H ≥ 0.5 and *A'* ≥ 0.75.

176 During the first 10 sessions, each rat was required to complete three sessions in a row
177 successfully, or training was stopped. Once the animal had reached this level of performance,
178 the second phase of the task began, in which we determined the smallest modulation depth
179 for which the rat discriminated between CS+ and CS-. Each session was split into two parts: an
180 initial "recall phase", during which the animal had to discriminate between 0% and 100%

modulated white noise for 20 random presentations of CS+ and CS-, followed by a test phase, during which the animal had to discriminate between 0% and a particular modulation depth: 80%, 60%, 40%, or 20%. Only one value of the modulation depth was used in this second part of the session, consisting of the highest modulation depth for which the animal did not yet complete a successful session. The animal had a maximum of three sessions to perform successfully at a given modulation depth before a lower modulation depth was selected. If the animal satisfied this criterion, a lower modulation depth was tested at the next session. If the animal did not satisfy the criterion after three sessions, or it satisfied this criterion only at the lowest modulation depth (20%), training was stopped.

Extracellular recordings in the primary auditory cortex

Acoustic stimuli

Acoustic stimuli were generated in Matlab, transferred to an RP2.1-based sound delivery system (TDT) and sent to a Fostex speaker (FE87E). The speaker was placed 2 cm away from the right ear of the rat. At this distance, the speaker produced a flat spectrum (± 3 dB) between 140 Hz and 36 kHz after calibration. The speaker was calibrated in a similar fashion to the A8X speaker, using noise to estimate the transfer function of the speaker. The inverted transfer function was applied to all sounds sent to the speaker. Spectrotemporal receptive fields were determined with 97 gamma-tone frequencies (the product of a gamma distribution and sinusoidal tone (Lyon et al. 2010)), covering eight octaves (0.14-36 kHz), presented in a random order at a rate of 4.15 Hz and at 75 dB SPL. The frequency response area was determined with the same set of tones presented from 75 to 5 dB SPL (5 dB steps, random order) at a rate of 2 Hz. Each tone was presented eight times at each intensity.

We quantified the responses to a set of heterospecific guinea pig vocalizations, corresponding to three representative examples of a whistle call used in a previous study (Gaucher et al. 2013), concatenated into a one-second stimulus presented 25 times. The vocalization was presented with and without two levels of white noise (60 and 70 dB SPL). We then used a gap detection protocol, involving a 300 ms guinea pig whistle (the first call from the set of three used above), split into two halves separated by a gap of 2, 4, 8, 16, 32 or 64 ms of silence. A 1 ms ramp was used at the transition between vocalization and the silent gap, on both sides of the gap. We used 25 repetitions of the stimulus for each of the six gap values.

Responses to amplitude-modulated white noise were tested with 15 presentations of 100% modulated white noise, at 2 Hz to 50 Hz. The first and second cycles of modulated white noise were also used to study the impact on (i) rising time and (ii) on forward suppression, respectively. Responses to modulation depth were assessed with 20 presentations of one second of white noise at 4 Hz, with a modulation depth ranging from 0% to 100%. We also used 30 repetitions of a 50 ms chord (inter-stimulus interval 150 ms) including a tone at 4 kHz and its harmonics of equal amplitude up to 40 kHz inserted in progressively decreasing white noise (the decrease in noise SPL over time was linear). The signal-to-noise ratio ranged from +16 dB to -16 dB over 6 seconds of stimulus. This stimulus was repeated 30 times. We also used 5 minutes of the random double sweep (RDS) stimulus previously designed by our team (Gourévitch et al. 2015).

Surgical procedure

The animal received an initial dose of ketamine and xylazine (100 mg/kg i.p. and 15 mg/kg i.p., respectively) supplemented with lower doses of ketamine (20 mg/kg) and xylazine (4 mg/kg) until reflex movements were no longer observed when the hind paw was pinched.

Liberal amounts of a local anesthetic (2% xylocaine) were injected subcutaneously into the skin above the skull and the temporal muscles. The animal was placed in a stereotaxic frame, a craniotomy was performed above the left temporal cortex, and the temporal bone was placed in sterile saline. The opening was 9 mm wide and began at the point of intersection between the parietal and temporal bones, at a height of 5 mm (Manunta and Edeline 1997, 1998, 2004). The dura above the auditory cortex was carefully removed under binocular control without damaging the blood vessels. At the end of surgery, a pedestal was built with dental acrylic cement, to fix the animal's head without the earbars during the recording session. The stereotaxic frame supporting the animal was placed in a sound-attenuating chamber (IAC, model AC1).

Recording procedure

Data were collected from multiunit recordings in the core auditory cortex (AC, primary auditory area AI, and anterior auditory field AAF). Extracellular recordings were obtained from arrays of 16 tungsten electrodes (ø: 33 µm, <1 MΩ) composed of two rows of eight electrodes separated by 1000 µm (350 µm between electrodes of the same row). A silver wire, used as the ground electrode, was inserted between the temporal bone and the dura mater on the contralateral side. The estimated location of AC was 4-7 mm posterior to bregma and 3 mm ventral to the superior suture of the temporal bone (corresponding to the area of interest, AI, defined by Paxinos and Watson (Paxinos and Watson 2005)). The raw signal was amplified by a factor of 10,000 (TDT Medusa) and processed by a multichannel data acquisition system (TDT RX5). The signal collected from each electrode was filtered (610-10,000 Hz) to extract multi-unit activity. The trigger level was carefully set for each electrode so as to select the largest action potentials from the signal. Online and offline examinations of the waveforms suggested

that the multi-unit activity collected here consisted of action potentials generated by three to six neurons close to the electrode. At the beginning of each recording session, we set the position of the electrode array such that the two rows of eight electrodes could sample neurons responding to low to high frequencies in the rostro-caudal direction (see example in Supp. Fig. 3ci).

Recording session

The recording depth was 300-700 µm, corresponding to layer III/IV and the upper part of layer V (Games and Winer 1988; Roger and Arnault 1989). We therefore mainly recorded the largest excitatory pyramidal neurons of layers III and V (Games and Winer 1988; Humphrey and Schmidt 1990; Smith and Populin 2001). Acoustic stimuli were presented at 75 dB SPL in the following order: gamma-tones to determine the pure tone spectrotemporal receptive field ($STRF^{pt}$, 5 min), followed by the frequency response areas (12 min), followed by the different sets of vocalizations without noise (3 min) and with increasing noise levels (60, 70 dB SPL, 3 min each). The gap detection protocol was then performed (3 min), followed by 3 min of spontaneous activity, and then the depth-modulated noise (4 min), amplitude-modulated noise (7 min), chords in noise (3 min), and the random double sweep (RDS, Gourévitch et al., 2015, 5 min) assessments. The presentation of this entire series of stimuli lasted 49 minutes. This set of stimuli was used with the electrode array positioned at two to five locations per animal, in the core auditory cortex.

Quantification of responses to pure tones

The $STRFs^{pt}$ derived from multi-unit activity were obtained by constructing post-stimulus time histograms (PSTHs) for each frequency, with 1 ms time bins. All $STRFs^{pt}$ were

smoothed with a uniform 5x5 bin window. The best frequency (BF) was then defined as the frequency at which the highest firing rate was recorded. A significant peak in the $STRF^{pt}$ was defined as a firing rate contour above the mean level of baseline activity (estimated from the first 10 milliseconds of $STRFs^{pt}$) plus six times the standard deviation of the baseline activity. For a given site, "bandwidth" was defined as the sum of all peak widths in octaves.

Other stimuli

We first constructed post-stimulus time histograms of the responses with a 2 ms time bin and a 5 ms uniform smoothing window. Individual examples for depth modulation transfer function, temporal modulation transfer function and gap detection are available in Supp. Fig. 4ai,aii,aiii. A significant peak in the PSTH was defined as a firing rate exceeding the mean + 4 standard deviations of the PSTH bin values corresponding to presumed spontaneous activity over a time interval of 100- to 300 ms (depending on the recording time for a given stimulus) starting 100 ms after the stimulus ended. Specific analyses were performed as follows.

Gap detection analysis

We considered the neural response to be modulated by the presence of the gap if an onset peak appeared in the PSTH, typically at the beginning of the second half of the vocalization, immediately after the gap. The peak was considered significant if its maximum amplitude was above the mean + 4 standard deviations of the PSTH values over a period of 50 ms immediately before the gap.

Analyses of temporal modulation transfer functions (TMTFs) and depth-MTFs.

TMTFs: for each modulation frequency or depth modulation, we calculated the vector strength (Goldberg and Brown 1969) (VS), defined as a measurement of the degree of phase-locking (or synchronization) of the spikes with the stimulus envelope. The VS ranged from 0 to 1. Depth-MTFs: for each modulation depth, we calculated the VS and took its value at the modulation frequency, 4 Hz.

Chords in noise analysis

We considered the neural response to be modulated by the presence of the chord if an onset peak appeared in the PSTH, typically within 0 to 100 ms after the beginning of acoustic stimulation. The peak was considered significant if its maximum amplitude was above the mean + 4 standard deviations of the spontaneous activity obtained in the period extending from 100 to 400 ms after the stimulus.

End of the recording session

After three to six hours of recording, the skull covering the temporal bone was carefully placed back over the auditory cortex and secured in place with a very thin layer of dental cement. The skin was cleaned and sutured to close the wound and an analgesic (buprenorphine, 0.05 mg/kg, s.c.) and an antibiotic (Convenia, 0.8 mg/kg, s.c.) were injected into the animal. The animal's health was monitored every six hours for 24 h, and the animal was kept in a separate cage for a few days before being returned to the colony room. After two to three weeks of recovery, the animals were sent to the INM (Montpellier) via a specialist transporter (Sanitrans, France), for peripheral auditory system assessment.

Peripheral auditory system assessments (DPOAEs, CAPs, ABRs)

Distortion product otoacoustic emissions (DPOAEs)

DPOAEs were used to assess the functional integrity of outer hair cells. DPOAEs were collected under anesthesia (a mixture of Zoletil 50 (tiletamine, 40 mg/kg) and Rompun (xylazine, 3 mg/kg)). They were recorded in the external auditory canal with an ER-10C S/N 2525 probe (Etymotic Research Inc. Elk Grove Village, IL, USA) consisting of two emitters and one microphone. The two primary tones were generated, and the distortion was processed by the Cubdis HID 40133DP system (Mimosa Acoustics, Champaign, IL, USA). The two tones were presented simultaneously, with f_2 sweeping from 0.5 kHz to 16 kHz in quarter-octave steps, and the maintenance of a constant f_2/f_1 ratio of 1.2. The primary intensities of f_2 and f_1 were set to 60 and 55 dB SPL, respectively. For each frequency, the cubic distortion product $2f_1$-f_2 and the neighboring noise magnitudes were measured and expressed as a function of f_2.

Compound action potential (CAP) of the auditory nerve

Recordings were performed under anesthesia (Zoletil 50 (tiletamine, 40 mg/kg) and Rompun (xylazine, 3 mg/kg)) in a Faraday-shielded anechoic soundproof cage. Rectal temperature was measured with a thermistor probe, and maintained at 38 °C ± 1 °C with a heated blanket placed underneath the animal. Signals were generated, acquired and processed with an NI PXI-4461 signal generator (National Instruments) controlled with LabVIEW software. Bursts of pure tones (1 ms rise/fall time, 10 ms duration, 11 bursts/s, 200 presentations per level, alternating polarity) were delivered by a JBL 075 loudspeaker (James B. Lansing Sound) positioned 10 cm away from the ear tested, in calibrated free-field conditions. Electrophysiological signals (×20,000) were amplified with a Grass P511 differential amplifier with a 300 Hz to 3.5 kHz bandpass.

The CAP of the auditory nerve was recorded from an electrode located in the round window niche (active) and two subcutaneous needle electrodes placed on the pinna of the ear tested and in the neck muscles (ground). Intensity-amplitude functions were obtained, at each frequency tested (1, 2, 4, 8, 16, 24, 32 kHz), by varying the intensity of the tone burst from 0 to 80 dB SPL, in 5 dB increments. CAP amplitude was measured between N1 and P1, with CAP threshold defined as the dB SPL required to elicit a measurable response of greater magnitude than the noise level.

Immunohistochemistry

Quantification of GAD67 labeling

At the end of the CAP recording session, the rats were deeply anesthetized with a mixture of ketamine and xylazine (200 mg/kg body weight and 15 mg/kg, respectively, i.p.) and transcardially perfused with 150 ml of saline and 1,000 ml of a fixative solution consisting of 4% paraformaldehyde (PFA) in 0.1 M phosphate buffer (pH 7.4). The brains were collected and fixed in 4% PFA; they were then incubated in incremental concentrations of sucrose (10, 20 and 30%). Each brain was sliced (40 µm sections) on a cryostat (HM55O, Microm, Thermo Fisher Scientific), from stereotaxic coordinates -4 mm to -6 mm relative to bregma (Paxinos and Watson 2009, 6^{th} edition). One in every four slices was stained with Nissl stain and three co-authors (JME, FO, ND) examined the stained coronal sections to select the anterior-posterior level corresponding to the center of the AI. One adjacent section (immediately before or after the Nissl-stained slice) was used for GAD67 labeling. The brain slices were rinsed in 1 x PBS and endogenous peroxidases were inactivated by incubation in 1 x PBS supplemented with 10% methanol and 10% H_2O_2. The coronal sections were then washed and permeabilized in 2.5% Triton X-100 in 1 x PBS (PBST). Nonspecific antigen sites were blocked by incubation with 5%

normal goat serum and 1% BSA in PBST. The sections were then incubated overnight at 4 °C with the primary anti-GAD67 antibody (Euromedex, GeneTex) diluted 1:500 in the same blocking solution. The sections were washed in PBST and incubated with a secondary antibody (biotinylated anti-rabbit IgG antibody, EuroBio) for two hours at room temperature. Staining was detected with an ABC kit (EuroBio), in accordance with the manufacturer's instructions. Sections were then mounted on glass slides (Fisher) in 0.3% PB gelatin. On the third day, slides were dehydrated and mounted in Eukitt (Fisher). Photomicrographs were taken with an upright optical microscope (Olympus BX60) equipped with mapping software (MercatorPro; ExploraNova, France). Immunolabeling was assessed in two predefined areas (800x300 µm) manually delimited in the center of the AI, in the supragranular and infragranular layers. The immunolabeled cells were counted by an experimenter blind to the age of the animal.

Number of ribbon synapses per inner hair cell along the tonotopic axis

The immunohistochemical method for assessing the number of synapses per inner hair cell (IHC) has been described in detail elsewhere (Bourien et al. 2014; Batrel et al. 2017). Briefly, the presynaptic IHC ribbons were identified with a mouse anti-CtBP2 antibody (1:500; BD Biosciences, San Diego, CA). Glutamate receptors were labeled with a mouse antibody raised against the C-terminus of the GluA2 subunit, IgG2a (1:200, Millipore, Billerica, MA). A 3D, custom algorithm was used to detect the juxtaposition of pre- and post-synaptic structures in stacked confocal images. Once the ribbons had been counted, the corresponding coding frequency of each ribbon was inferred from the rat cochlear place frequency map (Müller 1991). A second-order polynomial was then fitted to synapse count as a function of position relative to the cochlea apex (Meyer et al. 2009).

Statistical analysis

We mostly used ANOVA (one-way, two-way, three-way) to test for effects in our data. Stimulus parameters were systematically considered to be categorical in ANOVA. Most ANOVA tests were three-way, with exposure, exposure duration, and stimulus parameters as factors. The total number of observations used to compute the second degree of freedom of such ANOVA tests was therefore the number of animals, or cortical sites, for all groups (in Supplementary Table 1), multiplied by the number of stimulus parameters for each protocol, provided in Supplementary Table 2. In practice, it was lower than the theoretical maximum, as certain combinations were unavailable. Following significant ANOVA test results, post-hoc Student's *t*-tests were performed, without correction for multiple comparisons, for peripheral auditory system testing (*n* is small and stimulus parameters, such as frequency, typically take only a few values). Tukey-Kramer correction was used for cortical test results if the stimulus parameter could take more than four values.

The statistical distribution of many parameters, including firing rates, is typically skewed. We therefore applied a Log_{10} transformation to render these distributions Gaussian. The robustness of ANOVA to small deviations from normality (Lix et al. 1996; Blanca et al. 2017) and the large sample sizes of our groups (see Supplementary Table 1) ensured that ANOVA was a valid option. Furthermore, there is currently no satisfactory non-parametric solution for two-way and three-way tests.

Data and code availability

The datasets and code supporting the current study are available from the corresponding author on request.

Results

Lifetime exposure and synaptopathy

Noise in urban, professional and leisure environments typically consists of continuous broadband sounds with a low-pass temporal envelope (Supp. Fig. 1a-c). We designed a realistic random noise mimicking these spectrotemporal properties, to assess the effects of lifetime exposure to environmental noise on peripheral and central auditory processing (Fig. 1a). We then exposed young (three-month-old) adult Sprague-Dawley rats to such noise at 80 dB SPL, for 8 h per day over periods of 3, 6, 12 and 18 months (see suppl Table 1). By initiating exposure in adult rats, we avoided the massive effects of developmental plasticity, which occur during early exposure to noise (Barkat et al. 2011; de Villers-Sidani and Merzenich 2011; Bhumika et al. 2020). The longest period of exposure (18 months) covers 70 to 80% of the typical lifespan of Sprague-Dawley rats (680-760 days, see Davis et al. 1956; Durbin et al. 1966). Initial noise exposure occurred post-sexual maturity, which is around P60 for female Sprague-Dawley rats (Evans 1986). Although slightly exaggerated, our use of the word "lifetime" is consistent with previous human studies implicitly dealing with noise exposure that occurred mostly during adulthood (Prendergast et al. 2017; Valderrama et al. 2018). We analyzed the functional properties of the peripheral and central auditory system of these rats three weeks after the end of the exposure period, to investigate the long term, potentially permanent, effects (Fig. 1b). Specific aging effects were described in detail in a previous study on control animals from the same cohort (Occelli et al. 2019). Briefly, we found that aging effects were very limited at the periphery and moderate at the cortical level, also disfavoring any putative physiological effects related to ambient noise in the control animal facility (<30dB SPL in the rat hearing

range). Unless otherwise indicated, all ANOVAs were three-factor tests (exposure x exposure duration x stimulus parameter).

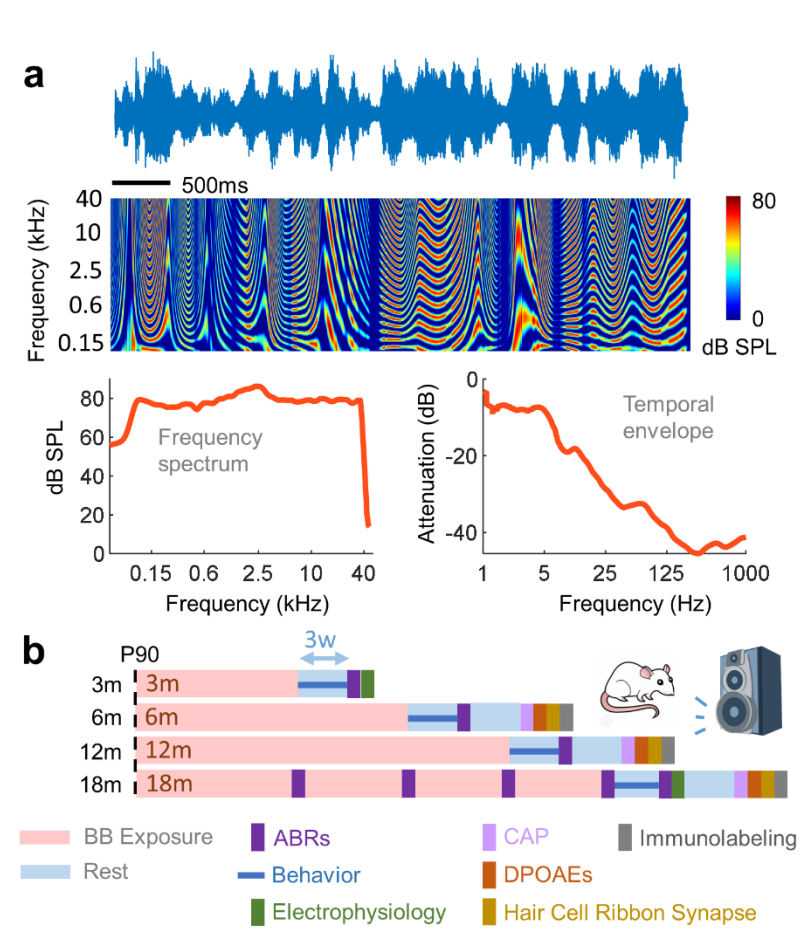

Fig. 1: Lifetime exposure to a realistic environmental noise. a *We designed a broadband sound based on amplitude-modulated dynamic moving ripples* (Kowalski et al. 1996; Escabi and Schreiner 2002). *A random low-pass temporal envelope was applied to match environmental sounds. The overall spectrum was flat, to ensure that no particular frequency band was favored.* ***b*** *Groups of P90 animals reared in a dedicated facility were exposed to this realistic noise for 3, 6, 12 or 18 months. The sound intensity in the cage of the animal was 80 dB SPL (Supplementary Fig. 1d). At the end of the exposure period, each animal was subjected to the following protocols, in the following order: a three-week behavior task; determination of auditory brainstem responses (ABRs); extracellular recordings in the primary auditory cortex; two weeks of rest; functional assessments of the peripheral auditory system (CAP, DPOAEs); immunolabeling of the cochlea and cerebral areas (see methods). For the animals exposed to noise for 18 months, ABRs were performed not only at the end of the exposure period, but also with no rest after 3, 6 and 12 months of exposure. The number of animals involved in each process is detailed in Supplementary Table 1.*

It has been shown that temporary threshold shifts (TTS) following exposure to loud sounds (e.g. 100 dB SPL) can be accompanied by a "synaptopathy": auditory thresholds return to normal after a few weeks, but the response of the auditory nerve decreases, as do the number of auditory fibers connected to inner hair cells and the distortion product otoacoustic emissions

(DPOAEs), all these effects being exacerbated by aging (Kujawa and Liberman 2009; Fernandez et al. 2015; Hickox et al. 2017). Here, we explored whether hearing loss and/or synaptopathy occurred after a lifetime of exposure to 80 dB SPL. We found that the auditory thresholds of exposed rats, as determined by auditory brainstem recordings (ABRs), were similar to those of age-matched control rats for all exposure durations, from 3 to 18 months (Fig. 2a, $F_{1,651}=1.99$, $p=0.16$), suggesting that lifetime exposure (beginning early in adulthood) did not cause permanent hearing loss. The largest ABR wave amplitudes were also unaffected (see Supp. Fig. 2b). Interestingly, the thresholds measured immediately after exposure, before the three-week rest period, were significantly higher after six and 12 months of exposure (and after 3 and 12 months of exposure for ABR amplitudes, see Supp. Fig. 2b), suggesting that these animals experienced a temporary threshold shift. After 18 months of exposure, this TTS was no longer significant, probably because the rats were more than 21 months old and their auditory thresholds had degraded due to aging, as previously shown (Occelli et al. 2019).

We then investigated the peripheral auditory system of the animals after 6, 12 and 18 months of exposure. We assessed the functional state of the outer hair cells by measuring DPOAEs. There was a significant interaction between the effects of noise exposure and exposure duration ($F_{2,1699}$=1167, p<1e-10, Fig. 2b), but discernible differences between the DPOAEs of exposed and control animals were rare and restricted to the 3-4 kHz range, in which the amplitude of DPOAEs is very low anyway. This suggests that noise exposure had little effect on outer hair cell function after exposure to noise for three months or a lifetime. For the N_1 wave of compound action potentials (CAPs), corresponding to wave I of ABRs and the activity of the auditory nerve, noise exposure increased thresholds (Fig. 2cii, $F_{2,243}$=880, p<1e-10) but, again, the magnitude of this effect was very modest (<10 dB for any frequency) and only significant at 4 kHz, after lifetime exposure. We found that latencies were longer (80 dB SPL, $F_{2,243}$=13.2,

481 p<1e-10; 40 dB SPL, $F_{2,243}$=8.4, p=3e-4, Fig. 2civ) and CAP amplitude was lower (80 dB SPL,
482 exposure factor, $F_{2,243}$=12.2, p=6e-4; 40 dB SPL, $F_{2,243}$=4.9, p=9e-3) at many frequencies, after
483 lifetime exposure (Fig 2ciii, and Fig2civ). Indeed, for all thresholds, latencies and amplitudes,
484 significant differences in post-hoc tests were found between control animals and animals
485 exposed to individual frequencies only after 18 months of exposure. Latencies were the most
486 widely affected parameter of CAPs (Fig2civ), and the effects of noise exposure were visible both
487 at suprathreshold (80 dB SPL) levels and at a lower level (40 dB SPL). In the presence of a
488 synaptopathy, these effects would be accompanied by a decrease in the number of synapses
489 per inner hair cell (IHC). We estimated the change in the number of synapses per IHC from a
490 3D reconstruction of pre- and post-synaptic structures in stacked confocal images (Fig. 2di).
491 Exposure to noise for 6 or 18 months had no effect on the number of synapses per IHC
492 ($F_{1,111}$=0.04, p=0.84, Fig. 2dii). Overall, these results suggest that the peripheral auditory system
493 of rats is remarkably robust to moderate noise exposure for at least 12 months.

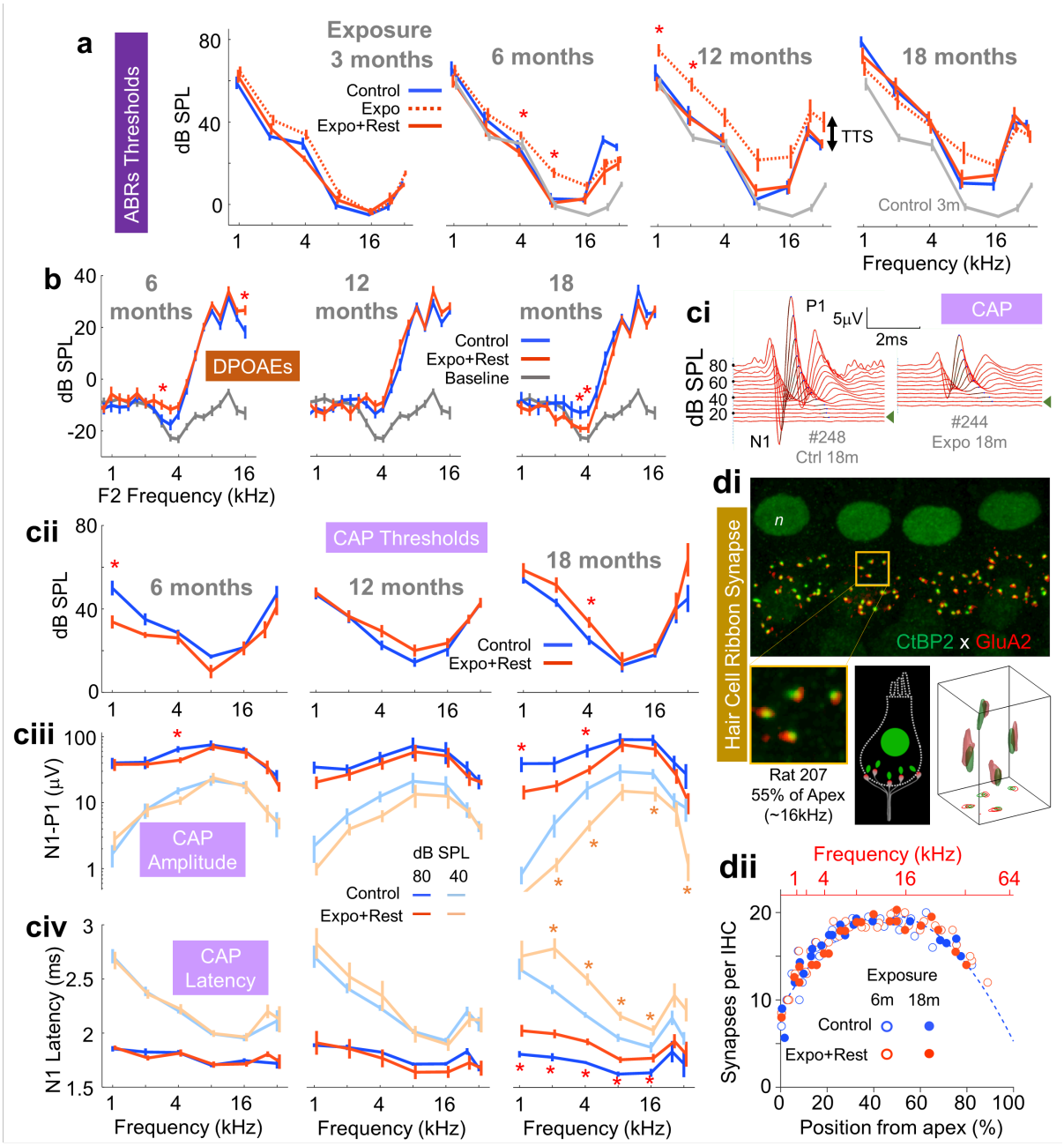

Fig. 2: Effects of broadband noise exposure on the peripheral auditory system. ***a*** *Average auditory thresholds obtained by auditory brainstem recordings (ABRs) for exposure durations of 3 (left) to 18 (right) months. There is a significant temporary threshold shift after 6 and 12 months of exposure (exposure factor, 3 months, $F_{1,215}$=3.63, p=0.06, 6 months, $F_{1,234}$=23.79, p<1e-10, 12 months, $F_{1,213}$=39.32, p<1e-10, 18 months, $F_{1,142}$=0.86, p=0.35, t-tests *p<0.05, for this and subsequent plots).* ***b*** *DPOAEs for exposure durations of 6, 12 and 18 months. The gray line indicates the noise level.* ***ci*** *Examples of CAP recordings obtained from a control animal (left) and an animal exposed (right) to noise at intensities ranging from 10-80 dB.* ***cii*** *CAP thresholds for exposure durations of 6, 12 and 18 months.* ***ciii*** *CAP amplitude at 80 dB SPL (dark colors) or 40 dB SPL (light colors) for exposure durations of 6, 12 and 18 months.* ***civ*** *CAP latency after noise exposure, presentation as in ciii.* ***di*** *Simultaneous labeling of presynaptic inner hair cell (IHC) ribbons with a mouse anti-CtBP2 antibody (green) and of postsynaptic glutamate receptors (GluA2 subunit, red). The lower left panel shows a magnification of labeling at the synaptic level. The lower central panel illustrates the theoretical expected juxtaposition of labeling for pre- and post-synaptic structures for a given hair cell. The lower right panel shows the use of a 3D, custom-developed algorithm to detect the juxtaposition of pre- and post-synaptic structures in stacked confocal images, and to identify the synapses for a given IHC.* ***dii*** *Number of synapses per IHC as a function of the position of the ribbon synapse along the cochlea (abscissa). The frequencies, corresponding to cochlear locations, are indicated on the top axis (red). Each dot represents the mean for six consecutive IHCs* (Bourien et al. 2014)*. The dashed curve is a second-order polynomial fit to all data (f(x) = -*

0.005x2+0.459x+8.5, r^2 > 0.9, where x is the position relative to the apex, expressed in percent). ***a,b,c*** *Error bars indicated the SEM.*

Cortical evoked response is affected by 3 months of moderate noise exposure

We used a battery of acoustic stimulations to investigate the effects of three to 18 months of exposure on the responses of auditory cortex neurons. Moderate noise exposure has already been shown to affect these neurons (Noreña et al. 2006; Zheng 2012; Zhou and Merzenich 2012; Thomas, Friedman, et al. 2019). Here, we derived the evoked-to-spontaneous firing rate ratio (ESR) as a "normalized" measurement of firing rate (Manunta and Edeline 1997; Novák et al. 2016; Pauzin and Krieger 2018). Furthermore, as firing rates typically have a skewed statistical distribution, we converted this distribution to a gaussian form by applying a $20Log_{10}$ transformation. The ESR is therefore expressed in dB. We provide a rationale for this choice in Supp. Fig. 3^{bis}b.

The tuning properties of cortical sites are classically characterized by determining the pure tone spectrotemporal receptive field ($STRF^{pt}$), defined as the time-frequency response of neurons to pure tones at 75 dB SPL (Fig. 3ai). The best frequency (BF) is that eliciting the highest firing rate. The distribution of BFs in our study was similar in all groups (Supp. Fig. 3b). Contrary to several previous studies (Noreña et al. 2006; Zheng 2012), we found no significant effect of our exposure regimen on tonotopy, i.e. on the topographic organization of BFs in the primary auditory cortex and the anterior auditory field (Supp. Fig. 3c). However, the ESR at and around the BF was reduced by three months of noise exposure ($F_{1,100213}$=137, p<1e-10*,* Fig. 3aii). This decrease was not due to a change in the evoked firing rate (Supp. Fig. 3a). Instead, it was due to the increase in (baseline) spontaneous firing rate observed after three months of noise exposure ($F_{1,1513}$=31.6, p<1e-10, t-tests in Fig. 3aiii, see also Supp. Fig. 3a). The lower ESR led to a decrease in the bandwidth of neurons, i.e. the range of frequencies to which cortical sites

responded ($F_{1,1625}$=39, p<1e-10, *t*-tests in Fig. 3aiii) and a degradation of cortical auditory thresholds (Supp. Fig. 3ei). By contrast, 18 months of noise exposure had no effect on ESR, bandwidth, cortical thresholds or the spontaneous activity of cortical sites (Fig. 3aii,aiii and Supp. Fig. 3eii).

We obtained similar results for ESR when pure-tone stimulation, as in $STRFs^{pt}$, was replaced by broadband white noise with different rising times (from 10 to 250 ms, Supp. Fig. 3fi and fii). These results were also confirmed with natural sounds, including a guinea pig whistle (Fig. 3bi). The mean response time revealed that the onset peak response occurring at each salient part of the whistle was lower in rats exposed to noise for three months than in unexposed rats of the same age ($F_{1,3200}$=66, p<1e-10, *t*-tests in Fig. 3bii). This decrease also applied to the post-onset parts of the neural response ($F_{1,3204}$=18.9, p<1e-10, Fig. 3bii). The results on the onset and post-onset responses were similar following the addition of 60 or 70 dB of noise to the vocalization. The addition of noise generally affected the onset more than post-onset part, as also illustrated by the mean response time in the presence of noise (Supp. Fig. 3^{bis}a). Here again, 18 months of exposure did not decrease, and indeed even increased the onset and post-onset ESR for all noise levels (except post-onset, 70 dB, Fig. 3bii). The similar post-onset ESR values between the three and 18 month groups for control animals is noteworthy, and suggests that the onset was heavily degraded by the 60/70 dB noise in older control animals, unlike the post-onset part.

We were intrigued by this finding that a lifetime of exposure to noise actually improves the ESR in the presence of noise. We pursued our investigations further, by testing the response to a chord (4 kHz tone and its harmonics, all with equal amplitude) presented in progressively decreasing levels of noise (Fig. 3ci). The signal-to-noise ratio (SNR) of this stimulus ranged from

559 -16 to +16 dB. A neural response to the chord emerged from the noise at a SNR of about -4/-5
560 dB in all groups (Fig. 3cii). As shown by the mean time and the grouped data, chord detection
561 was reduced by exposure to noise for many SNR values for animals exposed to noise for three
562 months ($F_{1,48449}$=175, p<1e-10, t-tests in Fig. 3cii), but not in the group of animals exposed to
563 noise for 18 months. Interestingly, there was no interaction between exposure to noise for
564 three months and SNR level ($F_{29,48449}$=1.4, p=0.07). In other words, exposure to noise for three
565 months decreased the ESR to the chord regardless of the SNR of the stimulus, thereby altering
566 the ability of cortical sites to detect a salient sound in noise. Surprisingly, lifetime exposure to
567 noise did not impair nor improve the ESR significantly in the presence of noise.

568 Overall, our results for all the artificial and natural stimuli described above suggest that
569 a relatively "short" exposure to noise of three months, frequently considered in published
570 studies to be quite a long period of exposure given the lifespan of rodents, alters the response
571 of the core auditory cortex by increasing spontaneous activity, consequently reducing the
572 "signal-to-noise ratio" of the evoked onset response to sounds. However, these effects tend to
573 disappear rather than increase with the duration of exposure, and are no longer detected after
574 18 months of exposure.

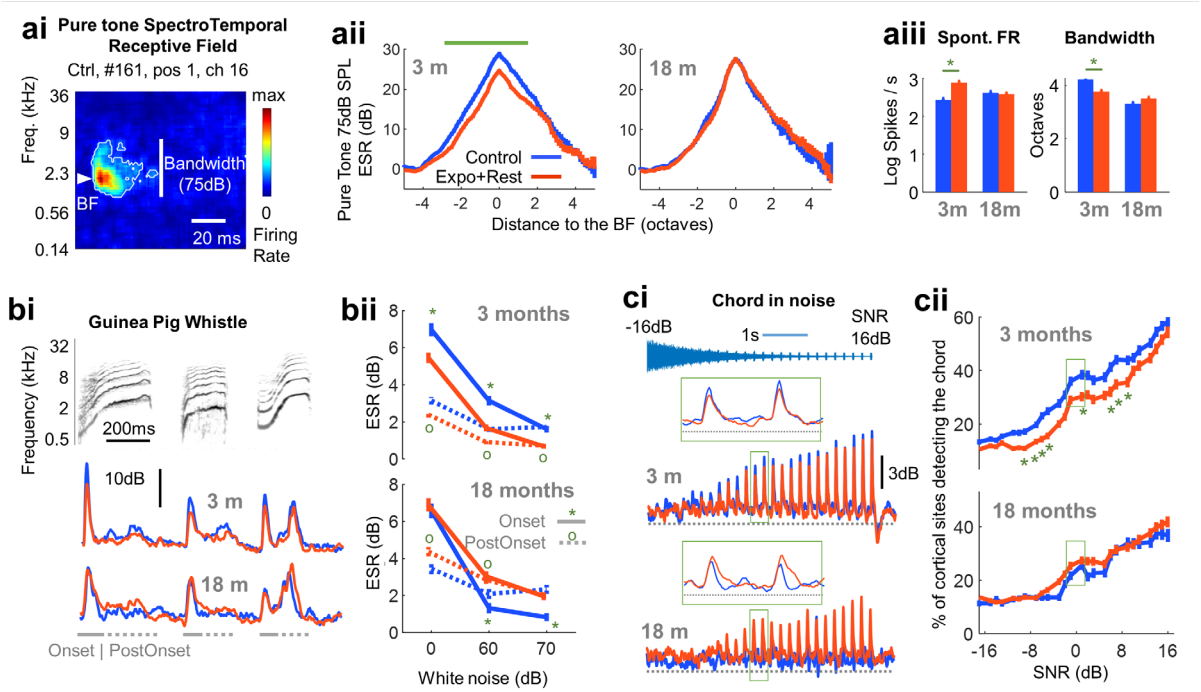

Fig. 3: Exposure to moderate noise for three months decreases the evoked response of the auditory cortex. ai *The spectrotemporal receptive field (STRF^{pt}) is the discharge rate of a cortical site as a function of frequency (y-axis) and time (x-axis) after acoustic stimulation with pure tones presented at 75 dB SPL. The best frequency of the cortical site (BF), i.e. the frequency eliciting the highest discharge rate, and the bandwidth (frequency band to which the cortical site responds) can be extracted from the STRF^{pt}.* ***aii*** *Averaged frequency profile of the STRF^{pt} (t-tests: p<0.05 for each frequency corresponding to the green line).* ***aiii*** *Spontaneous firing rate (left) and bandwidth of STRFs at 75 dB SPL (right). T-tests: *p<0.05, for this and all subsequent plots.* ***bi*** *Average response of all cortical sites from each group to three guinea pig whistles (represented by the spectrograms at the top). We distinguished the onset peak time intervals (gray solid line) from the post-onset time interval (gray dotted line). The onset response was reduced after three months, but not after 18 months of noise exposure.* ***bii*** *This result was statistically confirmed (see main text) by the quantification of onset and post-onset firing rates in response to the whistle in a background of silence or in the presence of background noise.* ***ci*** *Average response of cortical sites to a chord presented in progressively decreasing levels of noise. The peak value for the maximum response is reduced after 3 months of exposure for many noise levels, but not after 18 months. The green rectangles focus on the response for two levels of noise presented in the insets.* ***cii*** *Percentage of cortical sites showing a significant peak response to the chord in noise as a function of the signal-to-noise ratio (SNR) of the stimulus.*

Lifetime exposure degrades some temporal aspects of the cortical response

It was clear from our results (Fig. 3) that lifetime exposure affected the duration of the cortical response (see prolonged post-peak activities in the green rectangle in Fig. 3ci). We then investigated the temporal aspects of the cortical response (Fig. 4). We first showed that 18 months, but not three months, of noise exposure increased the duration of the peak response (see methods) to white noise bursts, which were either 250 ms ($F_{1,1625}$=6.4, p=0.01, t-tests in Fig. 4ai) or 100 ms long ($F_{1,1625}$=14.4, p=2e-4, t-tests in Fig. 4aii). We suspected that such an increase in the duration of the response might result from an exposure effect on neural

adaptation, and, thus, on the processing of sequences of acoustic events. A comparison of the ESRs to the first and second cycles of amplitude-modulated white noise showed that the (forward) suppression of the response to the second cycle was much stronger after 18 months than after three months of exposure ($F_{1,11295}$=92.6, p<1e-10, *t*-tests in Fig. 4b). We reasoned that this increase in forward suppression might affect the detection of short transients, such as gaps, by decreasing the post-gap neural peak response but it was not the case (Supp. Fig. 4b).

However, the increase in response duration affected the depth modulation transfer functions: after a lifetime of exposure, the ability of cortical neurons to distinguish 40%, 85% and 100% amplitude modulation in white noise ($F_{1,7571}$=9.5, p=2e-3, *t*-tests in Fig. 4c) was lower than that of unexposed animals. Could the changes in modulation depth processing be due to a decrease in the dynamic range of neurons, with cortical sites able to respond to a smaller range of intensity levels before reaching saturation? More non-monotonic rate-intensity functions were observed after a lifetime of exposure, but the overall slope and dynamic range extracted from these functions were not modified by exposure, irrespective of its duration (Supp. Fig. 4ci,cii,ciii,civ).

We then measured temporal modulation transfer functions, which track the phase-locking properties of neurons to various rates of amplitude modulation (Fig. 4d). We observed a decrease in the phase-locking abilities of neurons for fast modulation rates, between 14 and 24 Hz, after 18 months of exposure ($F_{1,14847}$=12.1, p=5e-4, *t*-tests in Fig. 4d). Consistent with our previous results on depth modulation processing (Fig. 4c) and forward suppression (Fig. 4b), this result suggests that the ability of neurons to follow temporal patterns in complex sounds is degraded by noise exposure. We addressed this hypothesis by computing, for each cortical site, the spectral coherence between spiking activity and the spectrogram of a complex

sound (the random double sweep, RDS, Gourévitch et al., 2015) taken at the BF of the cortical site (Fig. 4e). After a lifetime of exposure (but not after three months of exposure), we observed a massive decrease in the coherence between the RDS stimulus and the neural response, for most of the temporal modulation rates present in the stimulus ($F_{1,107315}$=470.4, p<1e-10, t-tests in Fig. 4e).

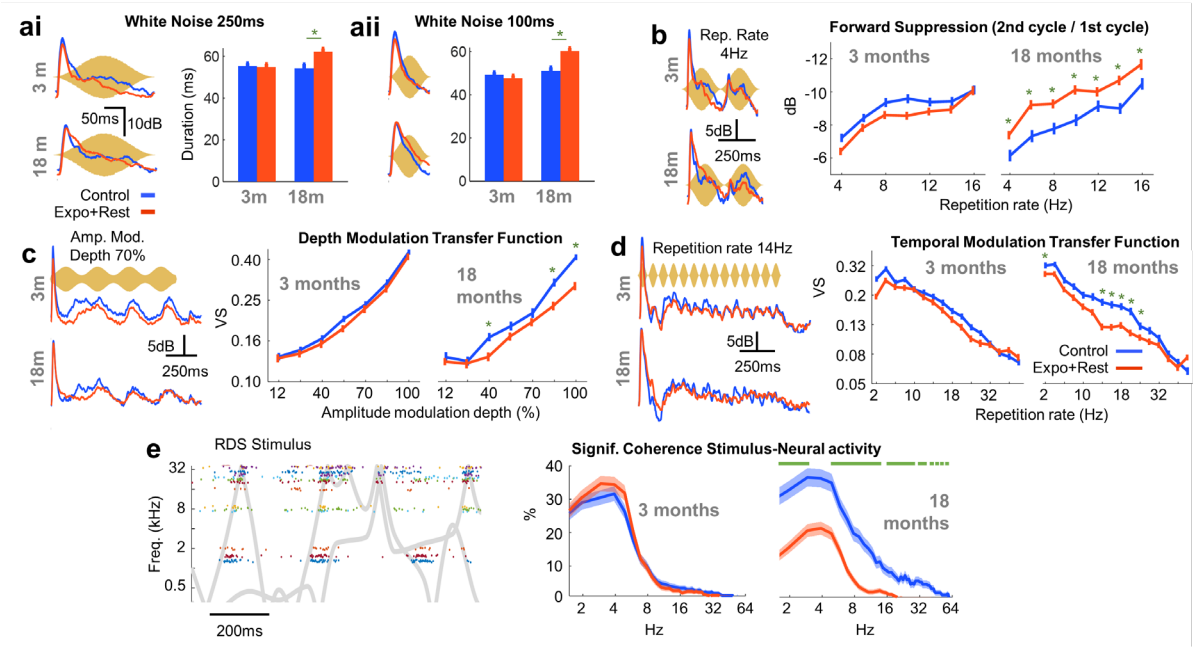

Fig. 4: Lifetime exposure to moderate noise affects the temporal response of the auditory cortex. ai *(left) Average response of all cortical sites to a 250 ms broadband white noise burst (125 ms rising time). (right) Quantification of the duration of the response evoked by a white noise stimulus lasting 250 ms. Post-hoc t-test: *p<0.05 as in all subsequent plots.* ***aii*** *As in ai for a 100 ms white noise stimulus.* ***b*** *(left) Average response of all cortical sites to two cycles of 250 ms broadband white noise bursts. (right) Quantification of forward suppression, estimated by calculating the ratio of the maximum firing rate evoked by the second cycle to that evoked by the first cycle.* ***c*** *(left) Average response of all cortical sites to four cycles of 250 ms broadband white noise bursts with a depth modulation of 70%. (right) Quantification of phase-locking, as measured by determining vector strength (VS) as a function of amplitude modulation depth.* ***d*** *(left) Average response of all cortical sites to white noise bursts repeated at a rate of 14 Hz. (right) Quantification of phase-locking, as measured by determining vector strength as a function of modulation rate, i.e. the neural temporal modulation transfer function (TMTF).* ***e*** *(left) A one-second excerpt of the response of 16 cortical sites to the random double sweep stimulus (RDS), the energy of which is represented in the time-frequency domain (kHz vs ms) in light gray. Each point is a spike and each cortical site is displayed at the ordinate corresponding to its best frequency, in its own color. (right) Percentage of neurons displaying significant coherence between the response of a cortical site and the spectrogram of the RDS taken at the best frequency of the cortical site, as a function of the temporal modulation rate of the stimulus. The green line indicates a significant difference between the two groups *p<0.05, t-test.*

These results indicate that, after a lifetime of noise exposure, cortical degradation affects the temporal aspects of neuronal responses and differs from the rate-related effects observed after three months of exposure.

Multidimensional analysis

The above findings were objectively quantified in a multidimensional analysis. We extracted 15 variables from previous analyses and standardized them (Fig. 5a). Exposure had an effect of similar magnitude on these variables in animals exposed to noise for three or 18 months (Fig. 5b). We also used this matrix of weakly correlated variables to build linear discriminant functions for distinguishing between our four experimental groups (3 months of exposure, 18 months of exposure, and unexposed animals of the same ages, Fig. 5c). Such discrimination was possible, as the rate of successful cortical site classification into the correct original group ranged from 40 to 50% (Fig. 5d). We then computed the mutual information (Fig. 5d, right) of each submatrix (black squares, Fig. 5d, left) associated with a duration of exposure. The mutual information was similar for both durations of exposure, implying that it was no easier to separate the cortical sites of exposed and unexposed animals after an 18-month exposure period than after a three-month exposure period, at least on the basis of our characterization of cortical activity. The linear discriminant function for distinguishing between the cortical sites of exposed and unexposed animals in the 18-month group (Fig. 5c) did not correlate with that of the three-month group (corr=-0.39, p=0.15). Overall, these results suggest that the cortical effects observed after 18 months of exposure were no stronger than or related to those observed after three months of exposure.

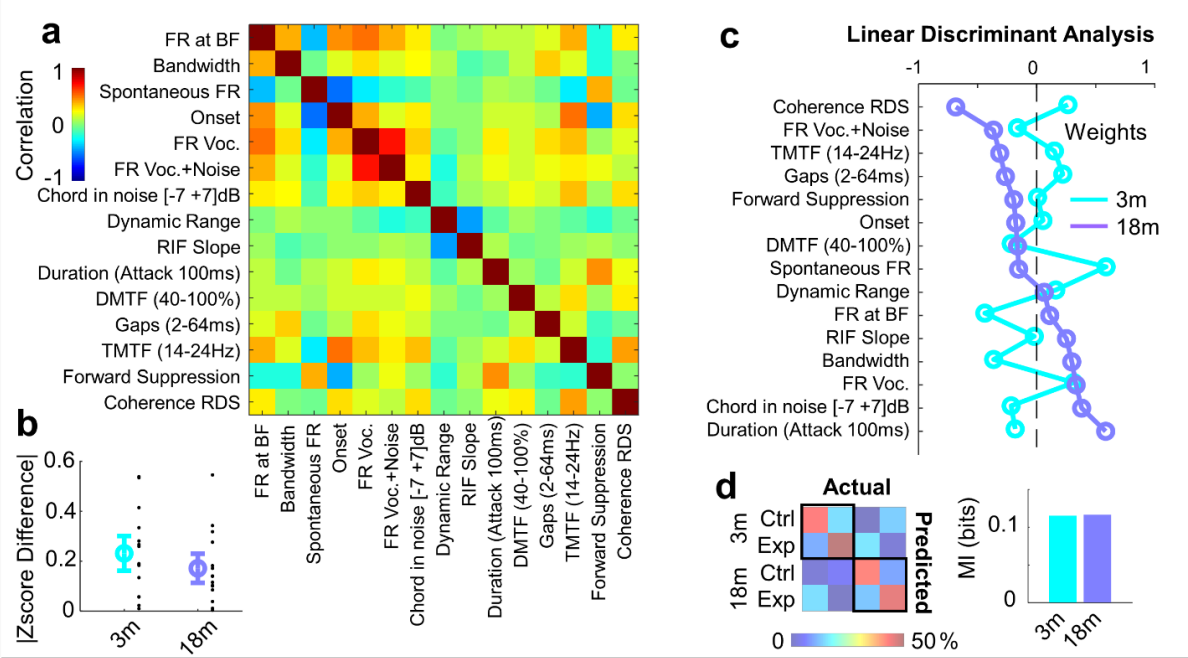

667

668 ***Fig. 5: The effects of lifetime and short-term exposure on the auditory cortex are orthogonal.*** ***a*** *Matrix of the*
669 *correlation between variables, summarizing the previous results (description at the end of the caption).* ***b*** *Z-score*
670 *difference in absolute values between exposed and unexposed animals for the 3-month and 18-month exposure*
671 *groups (t-test, T=-6.33, p=0.1).* ***c*** *Linear discriminant function: linear combination of the variables best separating*
672 *the cortical sites of exposed and unexposed animals from the three-month and 18-month exposure groups. Weights*
673 *are displayed and were sorted according to their contribution to the 18-month exposure function.* ***d*** *(left) Confusion*
674 *matrix obtained for the linear discriminant analysis displaying the classification of neurons achieved with the*
675 *parameters displayed in* ***a****. (right) Mutual information quantification of 2x2 submatrices (outlined in black) for each*
676 *duration of exposure. The variables were as follows: firing rate (FR) at BF: normalized FR at the BF (Fig. 3aii);*
677 *bandwidth: as in Fig. 3aiii; spontaneous FR: as in Fig. 3aiii; onset: as in Supp. Fig. 3fii averaged across all values of*
678 *rising slope; FR voc: FR response to vocalization as in Fig. 3 bii, 0dB noise; FR Voc. + Noise: onset response as in Fig.*
679 *3 bii, averaged between 60 and 70 dB of noise; chord in noise [-7 +7]dB: as in Fig. 3cii, averaged across SNR levels*
680 *between -7 and +7 dB, i.e. those with significant differences between exposed and unexposed cortical sites; dynamic*
681 *range: as in Supp. Fig. 4ciii; RIF slope: slope of rate-intensity function as in Supp. Fig. 4civ; duration (rising slope*
682 *100 ms): as in Fig. 4aii; DMTF (40-100%): depth modulation transfer function as in Fig. 4c, averaged across*
683 *modulation depth values between 40 and 100%; gaps (2-64 ms): as in Supp. Fig. 4b, averaged across gap durations*
684 *between 2 and 64 ms; TMTF (14-24 Hz): temporal modulation transfer function as in Fig. 4d, averaged across*
685 *modulation rates between 14 and 24 Hz; forward suppression: as in Fig. 4b, averaged across repetition rates*
686 *between 4 and 16 Hz; coherence RDS: as in Fig. 4e, averaged across frequencies between 1.5 and 16 Hz.*

687

688 Lifetime noise exposure does not degrade behavioral performance in a depth
689 modulation task

690 During the initial design of the protocol for this study, it was not possible to predict the
691 perceptive aspects potentially altered by lifetime exposure. We suspected that the prolonged
692 auditory masking undergone by animals due to noise exposure might affect their ability to

693 detect subtle changes in amplitude modulation. We thus decided to test the ability of animals
694 to detect low levels of depth modulation during a Go/NoGo task (Fig. 6a-b), using white noise
695 with the same amplitude modulations as in Fig. 4c. The findings reported above suggest that
696 the neural representation of modulation depth in the core auditory cortex is significantly
697 degraded by lifetime exposure to noise (see Fig 4c).

698 Behavioral experiments generated two results inconsistent with this view. First, the ability to
699 learn the task with a modulation depth of 100% was unaffected by exposure to noise,
700 regardless of its duration (Fig. 6c, exposure effect, $F_{1,68}$=0.06, p=0.8; interaction exposure and
701 duration of exposure, $F_{3,68}$=0.6, p=0.62). We detected an age-related deficit in learning ability
702 in both groups (duration of exposure, $F_{3,68}$=3.3, p=0.025; see also our previous study Occelli et
703 al. 2019). Second, although the number of animals that successfully learned the task (with our
704 criteria, see Methods) was limited (19/39 in the control group and 17/37 in the exposed group),
705 these animals had slightly better performances for discriminating small variations of depth
706 modulation after 3, 6, 12 and 18 months of exposure to noise (Fig. 6d, Supp. Fig. 6b). This
707 slightly better performance did not seem to be related to motor abilities, as the latency of
708 motor responses to the CS+ stimulus was similar in exposed and unexposed animals (Supp. Fig.
709 6c). This result contrasts sharply with those for electrophysiology. Actually, we found that the
710 behavioral output of a given animal (success or failure) was not dependent on the mean phase-
711 locking level measured in the neural population for the animal concerned, regardless of
712 amplitude modulation depth or noise exposure status (Fig. 6e).

713 The above results suggest that either a few months or a lifetime of noise exposure does not
714 adversely affect the detection and discrimination of amplitude modulation depth, despite its
715 degraded neural representation in the auditory cortex.

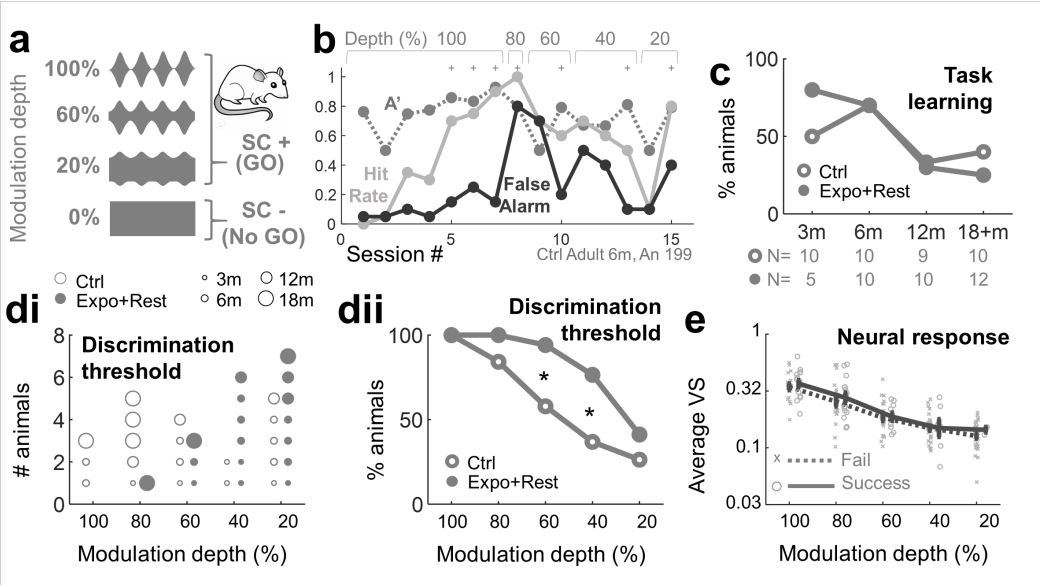

Fig. 6: Depth modulation perception is not damaged by long-term noise exposure. ***a*** *The behavioral task was an aversive Go-NoGo protocol in a shuttle box. The animal had to discriminate between noise with (SC+, Go) and without (SC–, NoGo) amplitude modulation at 4 Hz, the level of depth modulation varying between 20 and 100% (the same stimulus as that used to test neuronal responses, see Fig. 4c).* ***b*** *Individual example of a learning curve: first sessions include only a depth modulation of 100% to enable the animal to learn the task, a condition considered to be achieved after three successive sessions with an A' value >0.75. Depth modulation was then progressively decreased until A'>0.75 for a session. Failure in three successive sessions was the criterion for stopping the task. The threshold was defined as the last depth modulation successfully achieved.* ***c*** *Percentage of animals that were able to learn the task.* ***di*** *For the animals that successfully learned the task at a modulation depth of 100%, the threshold of depth modulation for each animal is shown as a circle, the diameter of which is proportional to exposure duration. For animals able to learn the task, noise-exposed animals (filled circles) had slightly better discrimination thresholds than those unexposed to noise.* ***dii*** *Percentage of animals achieving correct discrimination. Exposure facilitated discrimination, whatever its duration (three-way ANOVA: exposure, exposure duration, modulation depth, $F_{1,152}$=14.9, p=2e-4). The hypothesis of a normal distribution of the residuals for this model could not be rejected (Supp. Fig. 6a). Data for each exposure duration are shown in Supp. Fig. 6b. The percentage difference between exposed and unexposed animals was significant for modulation depths of 60% and 40% (proportion test, p=0.012, p=0.017 respectively,"*" in the plot).* ***e*** *Average VS of neurons as in Fig. 4c for all groups and for animals that failed (dotted curve, round markers) or succeeded (plain curve, cross markers) in the behavioral task for each amplitude modulation depth. No relationship was found between the behavioral output of the animal and the mean VS of neurons from the auditory cortex (four-way ANOVA: exposure, exposure duration, modulation depth, and behavioral output; behavioral output effect, $F_{1,4952}$=2.2, p=0.14; interaction exposure and behavior, $F_{1,4952}$=1.1, p=0.3; interaction modulation depth and behavior, $F_{4,4952}$=1.2, p=0.31).*

Discussion

Prolonged or lifetime exposure to a daily noise dose of 80 dB SPL has long been considered to result in a negligible or no permanent threshold shift in humans (ISO 1990; Lawton 2001) and animals (Canlon and Fransson 1995; Noreña et al. 2006; Liu et al. 2020). Consistent with expectations, we detected no permanent threshold shift (greater than expected for age) in rats, even after a lifetime of exposure. As levels known to lead to noise-induced hearing loss are

similar in rats and humans (Chen et al. 2014), this result may be considered to validate current employment regulations in industrial countries, which recommend the use of hearing protection at noise levels above 80 dB SPL.

Nonetheless, the level of exposure tested here, 80 dB SPL daily, may induce a negligeable TTS (0-5 dB) in humans (Ward et al. 1976). It has been suggested that noise below a particular SPL will produce no TTS, no matter how long an individual is exposed; this SPL, known as "effective quiet" (Ward et al. 1976) has been estimated at between 76 and 78 dB(A) in humans (Ward et al. 1976; Stephenson et al. 1980; Mills et al. 1981) and 77 dB SPL in rats (Chen et al. 2014). In both humans and rats, 80 dB(A) or SPL, respectively, generates a very small TTS that rapidly disappears. In addition, the TTS is thought to reach an asymptote after a few hours to days of exposure at moderate levels (Viall and Melnick 1977; Woodford 1977). Contrary to these hypotheses, we found here that a TTS can emerge (even after more than three months of exposure without TTS), then increase between 6 and 12 months of exposure, and subsequently becoming masked by the age-related threshold shift after 18 months of exposure (Fig. 2a). Protective mechanisms, such as the medial olivocochlear reflex, may become weaker, or the mechanisms associated with "ear toughening" (Niu and Canlon 2002) may become less efficient over time. Alternatively, a TTS associated with moderate noise exposure may trigger damage to the auditory system that accumulates over time. Indeed, mechanisms underlying TTS observed with louder sounds (>100 dB SPL) involve several inner ear sensorineural structures, including hair cells and their stereocilia, supporting cells within the organ of Corti, endothelial cells and fibrocytes within the stria vascularis and spiral ligament, as well as dendritic processes of the auditory nerve, through mechanical overstimulation, excitotoxicity and inflammatory processes (Mulroy et al. 1990; Puel et al. 1998; Nordmann et al. 2000; Henderson et al. 2006; Kujawa and Liberman 2009), all potentially contributing to so-called "hidden hearing loss" or

770 synaptopathy (Kujawa and Liberman 2015). It is, thus, crucial to determine whether moderate
771 noise-induced and synaptopathic noise-induced TTS have functional and anatomical
772 phenotypes in common.

773 The main phenotype (and definition) of synaptopathy is a loss of synapses between the IHCs
774 and spiral ganglion neurons (Kobel et al. 2017). Several studies have demonstrated
775 synaptopathy in rat models (Singer et al. 2013; Altschuler et al. 2016, 2019; Hickox et al. 2017),
776 including the Sprague-Dawley strain. However, we observed no such loss of synapses at any
777 cochlea location in our animals exposed to noise for 6 or 18 months (Fig. 2dii). It has been
778 suggested that a fine line at about 90 dB SPL separates neuropathic and non-neuropathic TTS
779 (Fernandez et al. 2015; Jensen et al. 2015). Consistent with this absence of synaptopathy, the
780 aging-related auditory threshold shift was not accelerated by lifetime exposure in the same way
781 as it is after synaptopathic events or early traumatic exposure (Kujawa and Liberman 2006;
782 Fernandez et al. 2015). If similar mechanisms are at work in rats and humans, our results
783 suggest that the workers in industrial countries protected by regulations limiting noise
784 exposure are unlikely to suffer from synaptopathy. Our results also suggest that the wave I
785 amplitude assay does not necessarily provide a reflection of underlying synaptic health
786 (Fernandez et al. 2015) or massive TTS (Lobarinas et al. 2017): a permanent decrease in CAP
787 amplitude (Fig. 2ciii) was observed in the presence of moderate TTS and absence of
788 synaptopathy.

789 DPOAEs were not affected by lifetime exposure in our conditions, suggesting that outer hair
790 cell functioning was intact or that there was a only a transient decrease in DPOAE amplitude
791 after noise exposure (Zhao et al. 2018). Nevertheless, they do not seem to be associated with
792 synaptopathic phenotypes (Kujawa and Liberman 2015).

With the notable exception of the CAP decrease in magnitude, the peripheral auditory system was remarkably robust to lifetime noise exposure. Note, however, that female rodents are slightly less prone to acoustic trauma than males, possibly due to the role of estrogen signaling (Milon et al. 2018; Shuster et al. 2019; Lin et al. 2021). We investigated whether a similar robustness applied at the cortical level. The adult brain is much more resistant to experience-dependent plasticity than the juvenile brain (Keuroghlian and Knudsen 2007), but several studies have shown that prolonged exposures at non-traumatic levels can trigger massive, albeit reversible, plastic changes at the cortical level (Noreña et al. 2006; Pienkowski et al. 2011; Zheng 2012; Zhou and Merzenich 2012; Lau et al. 2015; Thomas, Guercio, et al. 2019; Thomas et al. 2020). Unlike Zheng (2012), we found no signs of tonotopy disruption in our animals, whatever the duration of exposure (Supp. Fig. 3c). Any tonotopy disruption is unlikely to have been completely reversed by the three-week rest period, as the time constants for such reversals are typically longer (Pienkowski and Eggermont 2012). Functional reorganizations may be absent because synaptic weight distributions were not “unbalanced” by our stimulus, which should elicit excitation patterns similar to those for which the network has long been shaped, unlike unmodulated white noise (Zheng 2012; Thomas, Friedman, et al. 2019), narrowband sounds (Noreña et al. 2006) or fast noise bursts (Zhou and Merzenich 2012; Lau et al. 2015). For instance, narrowband sounds may introduce an unbalanced excitation/inhibition pattern, resulting in a decrease in evoked activity within the stimulation band, closely associated with an increase in evoked activity outside that band (Noreña et al. 2006; Pienkowski et al. 2013).

It has been suggested that prolonged passive exposure can also alter GABAergic expression (Zhou et al. 2011; Zhou and Merzenich 2012), leading to a re-opening of the critical period favoring functional reorganization (Zhou et al. 2011; Thomas, Friedman, et al. 2019). In

particular, this unbalanced excitation/inhibition state can elicit maladaptive cortical plasticity, leading to auditory disorders, including tinnitus and hyperacusis, an unusual intolerance to moderate sound intensities (Thomas, Guercio, et al. 2019). Correlates for such disorders may involve decreases in the ratio of the mean and spontaneous firing rates (for tinnitus) or of the mean and maximum firing rates (for hyperacusis (Pienkowski Martin et al. 2014)). We found no neurophysiological sign of hyperacusis, such as an increased slope, in our neural rate-intensity functions (Supp. Fig. 4c). However, we observed an increase in spontaneous, but not evoked, activity after three months of exposure (Fig. 3aii,aiii; Supp. Fig. 3a), a possible correlate of tinnitus (Noreña and Eggermont 2003; Munguia et al. 2013). Previous passive exposure studies obtained the opposite result (Munguia et al. 2013; Pienkowski 2018), but were based on narrowband stimulation. After a lifetime of exposure, the increase in spontaneous activity was no longer detectable, which may appear counterintuitive. Indeed, the 18-month exposure group had been experiencing TTS for months, and the decrease in auditory input may trigger central plasticity (Roberts et al. 2010), as suggested by the frequent co-occurrence of hearing loss with tinnitus and hyperacusis. It is possible that any “re-opening” of a critical period (or imbalance in neural activity, as indicated by abnormal levels of spontaneous activity) remains limited in duration or to a particular age range. Consistent with this idea, we observed no change in GABA expression in the thalamocortical system after a lifetime of exposure (Supp. Fig. 7aii).

Beyond spontaneous activity, is the neural representation of sound modified by prolonged noise exposure? The available evidence is limited to rare electroencephalographic studies (Kujala et al. 2004; Brattico et al. 2005; Samelli et al. 2012). In our study, despite the limited peripheral effects, long-term (3 months) and lifetime (18 months) exposures to noise clearly affected sound processing in the auditory cortex in surprisingly different manners. The increase

841 in spontaneous activity in the three-month exposure group may have led to a deterioration of
842 detection thresholds in the auditory cortex (Buran et al. 2014). We observed such a
843 deterioration in experiments involving stimulation with chords inserted in increasing levels of
844 noise (Fig. 3c) as well as when measuring cortical auditory thresholds (Supp. Fig. 3e). This
845 deterioration applied to "onset" and post-onset responses, as shown by the response times to
846 vocalizations (Fig. 3b).

847 Cortical effects observed after 18 months of exposure did not correlate with those observed
848 after three months of exposure (Fig. 5). Indeed, and importantly, temporal deficits were
849 observed only after lifetime exposure: the evoked response tended to lengthen (Fig. 4a),
850 accounting for a poorer ability of neurons to respond accurately to auditory contrasts (Fig. 4b),
851 fast temporal amplitude modulations (Fig. 4d) and, more generally, complex acoustic temporal
852 variations (Fig. 4e). One possible mechanism for this would involve a decrease in GABAergic
853 inhibitory expression, but we observed no such decrease (Supp. Fig. 7aii). The occurrence of a
854 degradation of temporal representations over relatively long time scales of hundreds of
855 milliseconds (forward suppression and depth modulation transfer functions at 4 Hz, Fig. 4bc)
856 but not very short ones (gap detection, Supp. Fig. 4b) suggests that other mechanisms, such as
857 synaptic depression (Wehr and Zador 2005) and, more generally, short-term plasticity may be
858 involved. A few studies have suggested that short-term plasticity may deteriorate with aging
859 (Mostany et al. 2013; Singh et al. 2018). Lifetime exposure may have accelerated this
860 deterioration of short-term plasticity, by as yet undetermined mechanisms.

861 Does this degradation of temporal abilities translate into a deterioration of auditory
862 performance? We directly quantified the behavioral response to amplitude-modulated noise
863 with various modulation depths. The success rate of learning for our young rats was relatively

low relative to that observed in a previous similar study (Kelly et al. 2006). There are at least two main reasons for this: the number of sessions allowed for each rat to learn the task (10) was probably too small and we also underestimated the difficulty of escape-avoidance learning for rats in a two-way shuttle box where the safe and dangerous places are not perceptually different (Theios and Dunaway 1964; Moot et al. 1974; Denny 2010). Neverthless, we found that noise exposure had no effect on the ability to learn the task (Fig. 6c). For the animals able to learn the task at a modulation depth of 100%, noise exposure generally improved modulation depth behavioral thresholds (Fig. 6d). This result is surprising, because it contrasts with the generally good agreement between electrophysiological (cortical and subcortical) and perceptive measurements of temporal abilities (Zhou and Merzenich 2012; Bharadwaj et al. 2015). It is possible that other brain areas involved in task learning (e.g., hippocampus, striatum, prefrontal areas, amygdala) partially account for the behavioral performance in the task we used, especially during aging (Cabeza et al., 2002; Milshtein-Parush et al., 2017; Moran et al., 2014), such that the behavioral performance correlates less with the neural coding performed by auditory cortex neurons. It is also surprising that noise exposure could facilitate specific perceptive abilities, although such a phenomenon was already reported when testing is performed in a noisy environment on adult rats (Zheng 2012) or when rat pups are reared in the presence of noise (Homma et al. 2020). Given the limited number of animals able to learn the behavioral task at a modulation depth of 100% in this study, further investigations and attempts to replicate this finding are required. However, this finding also opens up intriguing possibilities that cannot currently be ruled out. For instance, long-term exposure may elicit mechanisms either enhancing the sound-in-noise detection or compensating for the degraded neural representation of sounds, as during aging (Parthasarathy et al. 2019; Anderson et al. 2020) or hearing loss (Fuglsang et al. 2020). The auditory cortex recordings made in this study

888 do not support the hypothesis of improvements in the use of circuits dedicated to modulation
889 depth coding (Ding et al. 2014; Slama and Delgutte 2015; Fuglsang et al. 2020). Compensatory
890 top-down attentional processes (Spitzer et al. 1988; Fritz et al. 2007) could not be tested here
891 under anesthesia. However, plastic changes altering gain or excitatory/inhibitory balance
892 (Eggermont 2017; Parthasarathy et al. 2019) could have occurred throughout the animal's life
893 as suggested by the recovery of ESR measurements between three and 18 months of exposure.
894 In any case, the maintenance of task-learning ability in animals exposed to noise is consistent
895 with the weak evidence (Kumar et al. 2012; Hope et al. 2013) or total lack of evidence (Stephens
896 et al. 2003; Grose et al. 2017; Prendergast et al. 2017; Guest et al. 2018; Füllgrabe et al. 2020)
897 for a degradation of temporal abilities and, more generally, an impairment of speech
898 perception in humans due to occupational or leisure exposure to noise.

899 Our study therefore reveals several new paradoxes. A lifetime of exposure to noise does not
900 lead to structural damage to the synaptic ribbons, at least in our experimental conditions.
901 However, there seems to be an impact on auditory nerve activity, and our findings indicate that
902 TTS can develop progressively after months of exposure to noise. These findings call into
903 question the view that repeated daily noise exposure, even at a moderate SPL, does not
904 damage auditory system function over a period of years. This view is implicit in the occupational
905 regulations of industrialized countries, which are based on a daily permissible noise exposure
906 limit (85 dB(A), 8 hours per day in general). In addition, lifetime exposure can progressively
907 degrade the central representation of sounds, without necessarily affecting perception
908 abilities, raising a new possibility of passive exposure-induced plasticity over very long-time
909 scales.

Funding

This work was supported by grants from the French *Agence Nationale de la Recherche* (ANR) to B.G. (ANR-15-CE37-0007) and J-M.E. (ANR-14-CE30-0019), from the Fondation pour l'Audition to BG and from the "Attractivité" program of Paris-Sud University (2012) to BG. FH received support from the Hearing Prosthetist Group "Entendre" (R12090FF).

Acknowledgments

The authors are particularly grateful to Aurélie Bonilla, Fabien Lhericel, Joel Lefêvre and Céline Dubois for taking care of the rat colony.

Author contributions

Conceptualization, Methodology, B.G, J-M.E, J.B; Investigation, F.O, F.H, J.B, B.G, N.D, B.W; Writing – Review & Editing, J.B, B.G, J-M.E; Funding Acquisition, Resources B.G, J-M.E, J-L.P.

Competing Interests

The authors declare no competing interests

References

Altschuler RA, Halsey K, Kanicki A, Martin C, Prieskorn D, DeRemer S, Dolan DF. 2019. Small Arms Fire-like noise: Effects on Hearing Loss, Gap Detection and the Influence of Preventive Treatment. Neuroscience, Hearing Loss, Tinnitus, Hyperacusis, Central Gain. 407:32–40.

Altschuler RA, Wys N, Prieskorn D, Martin C, DeRemer S, Bledsoe S, Miller JM. 2016. Treatment with Piribedil and Memantine Reduces Noise-Induced Loss of Inner Hair Cell Synaptic Ribbons. Scientific Reports. 6:30821.

Anderson S, Roque L, Gaskins CR, Gordon-Salant S, Goupell MJ. 2020. Age-Related Compensation Mechanism Revealed in the Cortical Representation of Degraded Speech. J Assoc Res Otolaryngol. 21:373–391.

Barkat TR, Polley DB, Hensch TK. 2011. A critical period for auditory thalamocortical connectivity. Nat Neurosci. 14:1189–1194.

Batrel C, Huet A, Hasselmann F, Wang J, Desmadryl G, Nouvian R, Puel J-L, Bourien J. 2017. Mass Potentials Recorded at the Round Window Enable the Detection of Low Spontaneous Rate Fibers in Gerbil Auditory Nerve. PLOS ONE. 12:e0169890.

Bharadwaj HM, Masud S, Mehraei G, Verhulst S, Shinn-Cunningham BG. 2015. Individual Differences Reveal Correlates of Hidden Hearing Deficits. J Neurosci. 35:2161–2172.

941 Bhumika S, Nakamura M, Valerio P, Solyga M, Lindén H, Barkat TR. 2020. A Late Critical Period
942 for Frequency Modulated Sweeps in the Mouse Auditory System. Cereb Cortex.
943 30:2586–2599.
944 Blanca MJ, Alarcón R, Arnau J. 2017. Non-normal data: Is ANOVA still a valid option?
945 Psicothema. 552–557.
946 Bourien J, Tang Y, Batrel C, Huet A, Lenoir M, Ladrech S, Desmadryl G, Nouvian R, Puel J-L,
947 Wang J. 2014. Contribution of auditory nerve fibers to compound action potential of
948 the auditory nerve. J Neurophysiol. 112:1025–1039.
949 Brattico E, Kujala T, Tervaniemi M, Alku P, Ambrosi L, Monitillo V. 2005. Long-term exposure
950 to occupational noise alters the cortical organization of sound processing. Clinical
951 Neurophysiology. 116:190–203.
952 Buran BN, von Trapp G, Sanes DH. 2014. Behaviorally gated reduction of spontaneous
953 discharge can improve detection thresholds in auditory cortex. J Neurosci. 34:4076–
954 4081.
955 Canlon B, Fransson A. 1995. Morphological and functional preservation of the outer hair cells
956 from noise trauma by sound conditioning. Hear Res. 84:112–124.
957 Chen G-D, Decker B, Krishnan Muthaiah VP, Sheppard A, Salvi R. 2014. Prolonged noise
958 exposure-induced auditory threshold shifts in rats. Hear Res. 317:1–8.
959 Chen T-J, Chen S-S. 1991. Generator study of brainstem auditory evoked potentials by a
960 radiofrequency lesion method in rats. Experimental Brain Research. 85:537–542.
961 Dalla C, Shors TJ. 2009. Sex differences in learning processes of classical and operant
962 conditioning. Physiol Behav. 97:229–238.
963 Davis RK, Stevenson GT, Busch KA. 1956. Tumor Incidence in Normal Sprague-Dawley Female
964 Rats. Cancer Res. 16:194–197.
965 de Villers-Sidani E, Merzenich MM. 2011. Lifelong plasticity in the rat auditory cortex: basic
966 mechanisms and role of sensory experience. Prog Brain Res. 191:119–131.
967 Denny MR. 2010. Escape-Avoidance Learning. In: The Corsini Encyclopedia of Psychology.
968 American Cancer Society. p. 1–1.
969 Ding N, Chatterjee M, Simon JZ. 2014. Robust cortical entrainment to the speech envelope
970 relies on the spectro-temporal fine structure. NeuroImage. 88:41–46.
971 Durbin PW, Williams MH, Jeung N, Arnold JS, Parrott MW, Davis T. 1966. Development of
972 Spontaneous Mammary Tumors over the Life-Span of the Female Charles River
973 (Sprague-Dawley) Rat: The Influence of Ovariectomy, Thyroidectomy, and
974 Adrenalectomy-Ovariectomy. Cancer Res. 26:400–411.
975 Eggermont JJ. 2017. Acquired hearing loss and brain plasticity. Hearing Research, Plasticity
976 Following Hearing Loss and Deafness. 343:176–190.
977 Eldred KM, Gannon WF, von Gierke H. 1957. A laboratory method for the study of acoustic
978 trauma. Laryngoscope. 58:465–477.
979 Escabi MA, Schreiner CE. 2002. Nonlinear spectrotemporal sound analysis by neurons in the
980 auditory midbrain. J Neurosci. 22:4114–4131.
981 Evans AM. 1986. Age at puberty and first litter size in early and late paired rats. Biol Reprod.
982 34:322–326.
983 Fay MP, Freedman LS, Clifford CK, Midthune DN. 1997. Effect of Different Types and Amounts
984 of Fat on the Development of Mammary Tumors in Rodents: A Review. Cancer Res.
985 57:3979–3988.

Fernandez KA, Jeffers PWC, Lall K, Liberman MC, Kujawa SG. 2015. Aging after Noise Exposure: Acceleration of Cochlear Synaptopathy in “Recovered” Ears. J Neurosci. 35:7509–7520.
Freedman LS, Clifford C, Messina M. 1990. Analysis of Dietary Fat, Calories, Body Weight, and the Development of Mammary Tumors in Rats and Mice: A Review. Cancer Res. 50:5710–5719.
Fritz JB, Elhilali M, David SV, Shamma SA. 2007. Auditory attention--focusing the searchlight on sound. Curr Opin Neurobiol. 17:437–455.
Fuglsang SA, Märcher-Rørsted J, Dau T, Hjortkjær J. 2020. Effects of Sensorineural Hearing Loss on Cortical Synchronization to Competing Speech during Selective Attention. J Neurosci. 40:2562–2572.
Füllgrabe C, Moody M, Moore BCJ. 2020. No evidence for a link between noise exposure and auditory temporal processing for young adults with normal audiograms. The Journal of the Acoustical Society of America. 147:EL465–EL470.
Games KD, Winer JA. 1988. Layer V in rat auditory cortex: projections to the inferior colliculus and contralateral cortex. Hear Res. 34:1–25.
Gaucher Q, Huetz C, Gourévitch B, Edeline J-M. 2013. Cortical inhibition reduces information redundancy at presentation of communication sounds in the primary auditory cortex. J Neurosci. 33:10713–10728.
Goldberg JM, Brown PB. 1969. Response of binaural neurons of dog superior olivary complex to dichotic tonal stimuli: some physiological mechanisms of sound localization. J Neurophysiol. 32:613–636.
Gourévitch B, Edeline J-M, Occelli F, Eggermont JJ. 2014. Is the din really harmless? Long-term effects of non-traumatic noise on the adult auditory system. Nat Rev Neurosci. 15:483–491.
Gourévitch B, Occelli F, Gaucher Q, Aushana Y, Edeline J-M. 2015. A new and fast characterization of multiple encoding properties of auditory neurons. Brain Topogr. 28:379–400.
Grose JH, Buss E, Joseph W. Hall III. 2017. Loud Music Exposure and Cochlear Synaptopathy in Young Adults: Isolated Auditory Brainstem Response Effects but No Perceptual Consequences: Trends in Hearing.
Guest H, Munro KJ, Prendergast G, Millman RE, Plack CJ. 2018. Impaired speech perception in noise with a normal audiogram: No evidence for cochlear synaptopathy and no relation to lifetime noise exposure. Hearing Research. 364:142–151.
Henderson D, Bielefeld EC, Harris KC, Hu BH. 2006. The role of oxidative stress in noise-induced hearing loss. Ear Hear. 27:1–19.
Hickox AE, Larsen E, Heinz MG, Shinobu L, Whitton JP. 2017. Translational issues in cochlear synaptopathy. Hearing Research, Noise in the Military. 349:164–171.
Homma NY, Hullett PW, Atencio CA, Schreiner CE. 2020. Auditory Cortical Plasticity Dependent on Environmental Noise Statistics. Cell Reports. 30:4445-4458.e5.
Hope AJ, Luxon LM, Bamiou D-E. 2013. Effects of chronic noise exposure on speech-in-noise perception in the presence of normal audiometry. The Journal of Laryngology & Otology. 127:233–238.
Humphrey DR, Schmidt EM. 1990. Extracellular Single-Unit Recording Methods. In: Boulton AA,, Baker GB,, Vanderwolf CH, editors. Neurophysiological Techniques: Applications to Neural Systems. Neuromethods. Totowa, NJ: Humana Press. p. 1–64.

ISO. 1990. Acoustics: Determination of occupational noise exposure and estimation of noise-induced hearing impairment (No. 1990–1999). International standard.
Jensen JB, Lysaght AC, Liberman MC, Qvortrup K, Stankovic KM. 2015. Immediate and delayed cochlear neuropathy after noise exposure in pubescent mice. PLoS ONE. 10:e0125160.
Jowa L, Howd R. 2011. Should atrazine and related chlorotriazines be considered carcinogenic for human health risk assessment? J Environ Sci Health C Environ Carcinog Ecotoxicol Rev. 29:91–144.
Kelly JB, Cooke JE, Gilbride PC, Mitchell C, Zhang H. 2006. Behavioral Limits of Auditory Temporal Resolution in the Rat: Amplitude Modulation and Duration Discrimination. Journal of Comparative Psychology. 120:98–105.
Keuroghlian AS, Knudsen EI. 2007. Adaptive auditory plasticity in developing and adult animals. Progress in Neurobiology. 82:109–121.
Kobel M, Le Prell CG, Liu J, Hawks JW, Bao J. 2017. Noise-induced cochlear synaptopathy: Past findings and future studies. Hearing Research, Noise in the Military. 349:148–154.
Kowalski N, Depireux DA, Shamma SA. 1996. Analysis of dynamic spectra in ferret primary auditory cortex. I. Characteristics of single-unit responses to moving ripple spectra. J Neurophysiol. 76:3503–3523.
Kujala T, Shtyrov Y, Winkler I, Saher M, Tervaniemi M, Sallinen M, Teder-Sälejärvi W, Alho K, Reinikainen K, Näätänen R. 2004. Long-term exposure to noise impairs cortical sound processing and attention control. Psychophysiology. 41:875–881.
Kujawa SG, Liberman MC. 2006. Acceleration of age-related hearing loss by early noise exposure: evidence of a misspent youth. J Neurosci. 26:2115–2123.
Kujawa SG, Liberman MC. 2009. Adding insult to injury: cochlear nerve degeneration after “temporary” noise-induced hearing loss. J Neurosci. 29:14077–14085.
Kujawa SG, Liberman MC. 2015. Synaptopathy in the noise-exposed and aging cochlea: Primary neural degeneration in acquired sensorineural hearing loss. Hear Res.
Kumar UA, Ameenudin S, Sangamanatha AV. 2012. Temporal and speech processing skills in normal hearing individuals exposed to occupational noise. Noise and Health. 14:100.
Lau C, Zhang JW, McPherson B, Pienkowski M, Wu EX. 2015. Long-term, passive exposure to non-traumatic acoustic noise induces neural adaptation in the adult rat medial geniculate body and auditory cortex. Neuroimage. 107:1–9.
Lawton BW. 2001. a noise exposure threshold value for hearing conservation (No. 01/52). Concawe.
Lin N, Urata S, Cook R, Makishima T. 2021. Sex differences in the auditory functions of rodents. Hearing Research. 108271.
Liu X, Li L, Chen G-D, Salvi R. 2020. How low must you go? Effects of low-level noise on cochlear neural response. Hearing Research. 392:107980.
Lix LM, Keselman JC, Keselman HJ. 1996. Consequences of Assumption Violations Revisited: A Quantitative Review of Alternatives to the One-Way Analysis of Variance F Test. Review of Educational Research. 66:579–619.
Lobarinas E, Spankovich C, Le Prell CG. 2017. Evidence of “hidden hearing loss” following noise exposures that produce robust TTS and ABR wave-I amplitude reductions. Hearing Research, Noise in the Military. 349:155–163.
Lyon RF, Katsiamis AG, Drakakis EM. 2010. History and future of auditory filter models. In: Proceedings of 2010 IEEE International Symposium on Circuits and Systems. Presented at the Proceedings of 2010 IEEE International Symposium on Circuits and Systems. p. 3809–3812.

Manunta Y, Edeline JM. 1997. Effects of noradrenaline on frequency tuning of rat auditory cortex neurons. Eur J Neurosci. 9:833–847.
Manunta Y, Edeline JM. 1998. Effects of noradrenaline on rate-level function of auditory cortex neurons: is there a “gating” effect of noradrenaline? Exp Brain Res. 118:361–372.
Manunta Y, Edeline J-M. 2004. Noradrenergic induction of selective plasticity in the frequency tuning of auditory cortex neurons. J Neurophysiol. 92:1445–1463.
Meyer AC, Frank T, Khimich D, Hoch G, Riedel D, Chapochnikov NM, Yarin YM, Harke B, Hell SW, Egner A, Moser T. 2009. Tuning of synapse number, structure and function in the cochlea. Nat Neurosci. 12:444–453.
Mills JH, Adkins WY, Gilbert RM. 1981. Temporary threshold shifts produced by wideband noise. J Acoust Soc Am. 70:390–396.
Milon B, Mitra S, Song Y, Margulies Z, Casserly R, Drake V, Mong JA, Depireux DA, Hertzano R. 2018. The impact of biological sex on the response to noise and otoprotective therapies against acoustic injury in mice. Biol Sex Differ. 9:12.
Moot SA, Nelson K, Bolles RC. 1974. Avoidance learning in a black and white shuttlebox. Bull Psychon Soc. 4:501–502.
Mostany R, Anstey JE, Crump KL, Maco B, Knott G, Portera-Cailliau C. 2013. Altered Synaptic Dynamics during Normal Brain Aging. J Neurosci. 33:4094–4104.
Müller M. 1991. Frequency representation in the rat cochlea. Hear Res. 51:247–254.
Mulroy MJ, Fromm RF, Curtis S. 1990. Changes in the synaptic region of auditory hair cells during noise-induced temporary threshold shift. Hear Res. 49:79–87.
Munguia R, Pienkowski M, Eggermont JJ. 2013. Spontaneous firing rate changes in cat primary auditory cortex following long-term exposure to non-traumatic noise: tinnitus without hearing loss? Neurosci Lett. 546:46–50.
Niu X, Canlon B. 2002. Protecting against noise trauma by sound conditioning. Journal of Sound and Vibration. 250:115–118.
Nordmann AS, Bohne BA, Harding GW. 2000. Histopathological differences between temporary and permanent threshold shift. Hear Res. 139:13–30.
Noreña AJ, Eggermont JJ. 2003. Changes in spontaneous neural activity immediately after an acoustic trauma: implications for neural correlates of tinnitus. Hear Res. 183:137–153.
Noreña AJ, Gourévitch B, Aizawa N, Eggermont JJ. 2006. Spectrally enhanced acoustic environment disrupts frequency representation in cat auditory cortex. Nat Neurosci. 9:932–939.
Novák O, Zelenka O, Hromádka T, Syka J. 2016. Immediate manifestation of acoustic trauma in the auditory cortex is layer specific and cell type dependent. Journal of Neurophysiology. 115:1860–1874.
Occelli F, Hasselmann F, Bourien J, Eybalin M, Puel JL, Desvignes N, Wiszniowski B, Edeline J-M, Gourévitch B. 2019. Age-related Changes in Auditory Cortex Without Detectable Peripheral Alterations: A Multi-level Study in Sprague–Dawley Rats. Neuroscience. 404:184–204.
Parthasarathy A, Bartlett EL, Kujawa SG. 2019. Age-related Changes in Neural Coding of Envelope Cues: Peripheral Declines and Central Compensation. Neuroscience, Hearing Loss, Tinnitus, Hyperacusis, Central Gain. 407:21–31.
Pauzin FP, Krieger P. 2018. A Corticothalamic Circuit for Refining Tactile Encoding. Cell Reports. 23:1314–1325.
Paxinos G, Watson C. 2005. The Rat Brain in Stereotaxic Coordinates. Elsevier Academic Press.

Pienkowski M. 2018. Prolonged Exposure of CBA/Ca Mice to Moderately Loud Noise Can Cause Cochlear Synaptopathy but Not Tinnitus or Hyperacusis as Assessed With the Acoustic Startle Reflex. Trends in Hearing. 22:2331216518758109.

Pienkowski M, Eggermont JJ. 2012. Reversible long-term changes in auditory processing in mature auditory cortex in the absence of hearing loss induced by passive, moderate-level sound exposure. Ear Hear. 33:305–314.

Pienkowski M, Munguia R, Eggermont JJ. 2011. Passive exposure of adult cats to bandlimited tone pip ensembles or noise leads to long-term response suppression in auditory cortex. Hear Res. 277:117–126.

Pienkowski M, Munguia R, Eggermont JJ. 2013. Effects of passive, moderate-level sound exposure on the mature auditory cortex: spectral edges, spectrotemporal density, and real-world noise. Hear Res. 296:121–130.

Pienkowski Martin, Tyler Richard S., Roncancio Eveling Rojas, Jun Hyung Jin, Brozoski Tom, Dauman Nicolas, Coelho Claudia Barros, Andersson Gerhard, Keiner Andrew J., Cacace Anthony T., Martin Nora, Moore Brian C. J. 2014. A Review of Hyperacusis and Future Directions: Part II. Measurement, Mechanisms, and Treatment. American Journal of Audiology. 23:420–436.

Prendergast G, Guest H, Munro KJ, Kluk K, Léger A, Hall DA, Heinz MG, Plack CJ. 2017. Effects of noise exposure on young adults with normal audiograms I: Electrophysiology. Hearing Research. 344:68–81.

Puel JL, Ruel J, Gervais d'Aldin C, Pujol R. 1998. Excitotoxicity and repair of cochlear synapses after noise-trauma induced hearing loss. Neuroreport. 9:2109–2114.

Roberts LE, Eggermont JJ, Caspary DM, Shore SE, Melcher JR, Kaltenbach JA. 2010. Ringing ears: the neuroscience of tinnitus. J Neurosci. 30:14972–14979.

Roger M, Arnault P. 1989. Anatomical study of the connections of the primary auditory area in the rat. J Comp Neurol. 287:339–356.

Samelli AG, Matas CG, Carvallo RMM, Gomes RF, Beija CS de, Magliaro FCL, Rabelo CM. 2012. Audiological and electrophysiological assessment of professional pop/rock musicians. Noise and Health. 14:6.

SCENIHR. 2008. Potential health risks of exposure to noise from personal music players and mobile phones including a music playing function. EU Scientific Committee on Emerging and Newly Identified Health Risks.

Schweinfurth MK. 2020. The social life of Norway rats (Rattus norvegicus). eLife. 9:e54020.

Shuster BZ, Depireux DA, Mong JA, Hertzano R. 2019. Sex differences in hearing: Probing the role of estrogen signaling. The Journal of the Acoustical Society of America. 145:3656–3663.

Singer W, Zuccotti A, Jaumann M, Lee SC, Panford-Walsh R, Xiong H, Zimmermann U, Franz C, Geisler H-S, Köpschall I, Rohbock K, Varakina K, Verpoorten S, Reinbothe T, Schimmang T, Rüttiger L, Knipper M. 2013. Noise-Induced Inner Hair Cell Ribbon Loss Disturbs Central Arc Mobilization: A Novel Molecular Paradigm for Understanding Tinnitus. Mol Neurobiol. 47:261–279.

Singh M, Miura P, Renden R. 2018. Age-related defects in short-term plasticity are reversed by acetyl-L-carnitine at the mouse calyx of Held. Neurobiol Aging. 67:108–119.

Slama MCC, Delgutte B. 2015. Neural Coding of Sound Envelope in Reverberant Environments. J Neurosci. 35:4452–4468.

Smith PH, Populin LC. 2001. Fundamental differences between the thalamocortical recipient layers of the cat auditory and visual cortices. Journal of Comparative Neurology. 436:508–519.
Spitzer H, Desimone R, Moran J. 1988. Increased attention enhances both behavioral and neuronal performance. Science. 240:338–340.
Stephens D, Zhao F, Kennedy V. 2003. Is there an association between noise exposure and King Kopetzky Syndrome? Noise and Health. 5:55.
Stephenson MR, Nixon CW, Johnson DL. 1980. Identification of the minimum noise level capable of producing an asymptotic temporary threshold shift. Aviat Space Environ Med. 51:391–396.
Theios J, Dunaway JE. 1964. One-way versus shuttle avoidance conditioning. Psychon Sci. 1:251–252.
Thomas ME, Friedman NHM, Cisneros-Franco JM, Ouellet L, de Villers-Sidani É. 2019. The Prolonged Masking of Temporal Acoustic Inputs with Noise Drives Plasticity in the Adult Rat Auditory Cortex. Cereb Cortex. 29:1032–1046.
Thomas ME, Guercio GD, Drudik KM, de Villers-Sidani É. 2019. Evidence of Hyperacusis in Adult Rats Following Non-traumatic Sound Exposure. Front Syst Neurosci. 13:55.
Thomas ME, Lane CP, Chaudron YMJ, Cisneros-Franco JM, Villers-Sidani É de. 2020. Modifying the Adult Rat Tonotopic Map with Sound Exposure Produces Frequency Discrimination Deficits That Are Recovered with Training. J Neurosci. 40:2259–2268.
Valderrama JT, Beach EF, Yeend I, Sharma M, Van Dun B, Dillon H. 2018. Effects of lifetime noise exposure on the middle-age human auditory brainstem response, tinnitus and speech-in-noise intelligibility. Hearing Research. 365:36–48.
Verde ME, MacMillan NA, Rotello CM. 2006. Measures of sensitivity based on a single hit rate and false alarm rate: the accuracy, precision, and robustness of d', Az, and A'. Percept Psychophys. 68:643–654.
Viall J, Melnick W. 1977. Asymptotic threshold shift in people with sensorineural hearing loss. Trans Sect Otolaryngol Am Acad Ophthalmol Otolaryngol. 84:459–464.
Ward WD, Cushing EM, Burns EM. 1976. Effective quiet and moderate TTS: Implications for noise exposure standards. The Journal of the Acoustical Society of America. 59:160–165.
Wehr M, Zador AM. 2005. Synaptic mechanisms of forward suppression in rat auditory cortex. Neuron. 47:437–445.
Willott JF, Bross L. 2004. Effects of prolonged exposure to an augmented acoustic environment on the auditory system of middle-aged C57BL/6J mice: cochlear and central histology and sex differences. J Comp Neurol. 472:358–370.
Woodford C. 1977. Asymptotic Noise-Induced Temporary Threshold Shift in Chinchilla Measured by the Auditory Evoked Response. Audiology. 16:11–20.
Zhao D-L, Sheppard A, Ralli M, Liu X, Salvi R. 2018. Prolonged low-level noise exposure reduces rat distortion product otoacoustic emissions above a critical level. Hearing Research. 370:209–216.
Zheng W. 2012. Auditory map reorganization and pitch discrimination in adult rats chronically exposed to low-level ambient noise. Front Syst Neurosci. 6:65.
Zhou X, Merzenich MM. 2012. Environmental noise exposure degrades normal listening processes. Nat Commun. 3:843.

1216 Zhou X, Panizzutti R, Villers-Sidani É de, Madeira C, Merzenich MM. 2011. Natural Restoration
1217 of Critical Period Plasticity in the Juvenile and Adult Primary Auditory Cortex. J
1218 Neurosci. 31:5625–5634.
1219

1220

Supplementary materials

Exposure	Behavior	AI	ABRs	ABRs (exposed, no rest)	CAP	DPOAEs	Immunochemistry (AC + MGB)	N cortical sites
3 months	10/5	9/10	10/9	17				449/427
6 months	10/10		10/10	18	7/9	8/9		
12 months	9/9		9/10	14	8/7	9/6		
18+ months	10/12 [a]	7/11	9/11	7	5/7	5/7	6/5	309/444

Table 1: *Number of animals (columns 2 to 8) and cortical sites (last column) for the different exposure duration groups (control/exposed). Ten animals per group (20 per group for 18+ months) were initially planned. However, a few animals died before, during or after surgery. Other animals were removed from the study because they developed mammary tumors.*

Protocol	ABR thresholds / amplitude CAP thresholds / amplitude / latency	DPOAEs	STRFs[pt]	Chords in noise	BFs distribution
Corresponding figures	Fig. 1a,cii,cii,civ Supp. Fig. 2b	Fig. 1b	Fig. 3aii	Fig. 3cii	Supp. Fig.3b
Stimulus parameters	7	18	127	30	10
Protocol	Cortical thresholds	Attack duration	Forward Suppression	Depth Modulation Transfer Function	Temporal Modulation Transfer Function
Corresponding figures	Supp. Fig. 3ei,eii	Supp. Fig. 3fii	Fig. 4b	Fig. 4c	Fig. 4d
Stimulus parameters	252	16	7	7	16
Protocol	Coherence RDS-Neural activity	Gap detection	Modulation depth		
Corresponding figures	Fig. 4e	Supp. Fig. 4b	Fig. 6e		
Stimulus parameters	129	6	5		

Table 2: *Number of stimulus parameters for the protocols used in the study.*

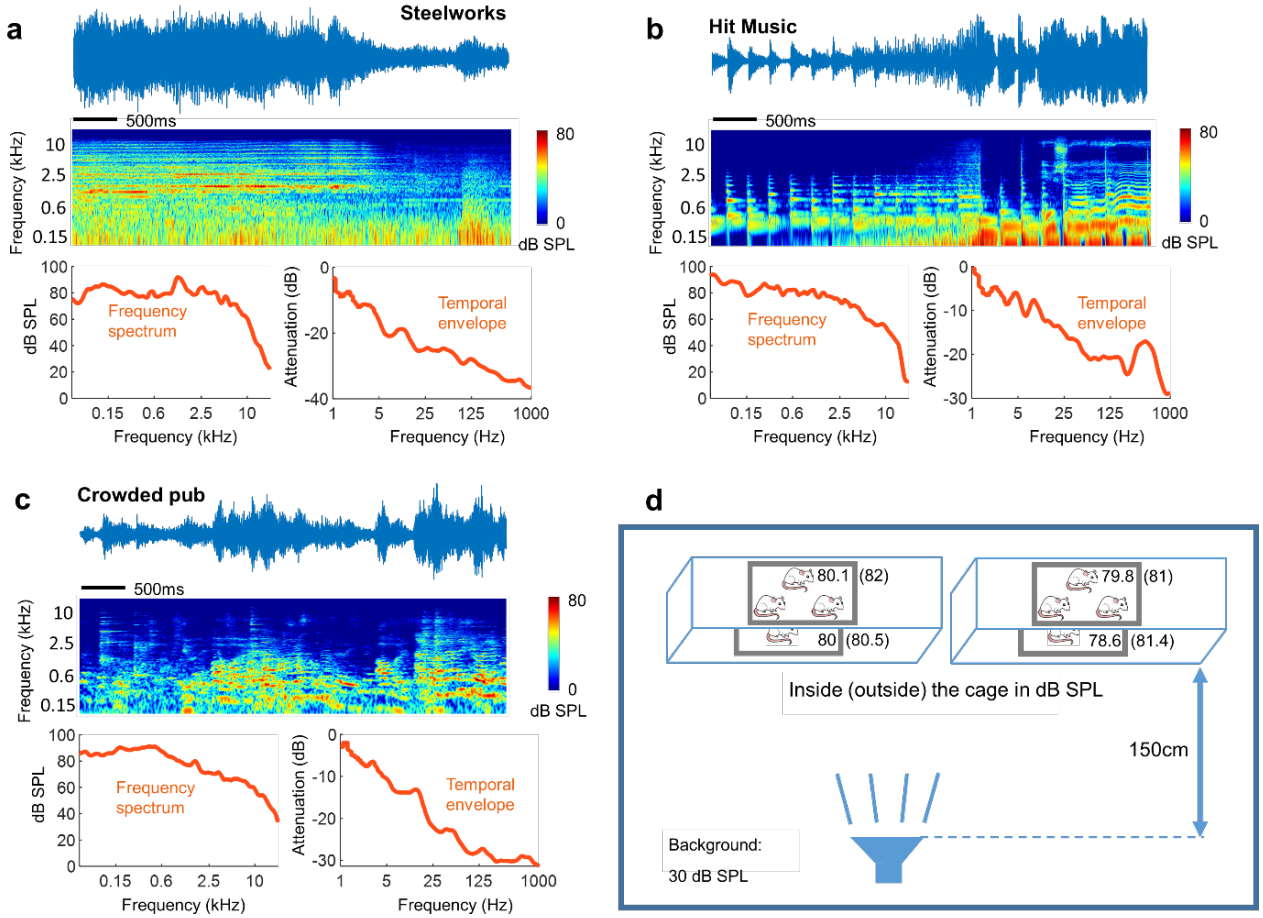

Supp. Fig. 1: a *As in Fig. 1a, acoustic signal (top), spectrogram (middle) and long-term frequency spectrum and temporal envelope spectrum of the stimulus (bottom) for a recording in steelworks (personal recording).* ***b,c*** *as for* ***a*** *but for hit music (David Guetta, Titanium) and a crowded pub (personal recording). All long-term frequency spectra of such sounds from our working or leisure sound environments are somewhat flat or slightly low-pass up to 10 kHz and the temporal envelope spectrum is typically low-pass with a predominance of amplitude modulations below 5-10 Hz.* ***d*** *Rats were placed in a dedicated soundproof chamber facing a large speaker. The sound delivery system was calibrated to achieve a flat spectrum inside the cages (which act as a natural low-pass filter) and the SPL was also carefully checked inside and outside the cages.*

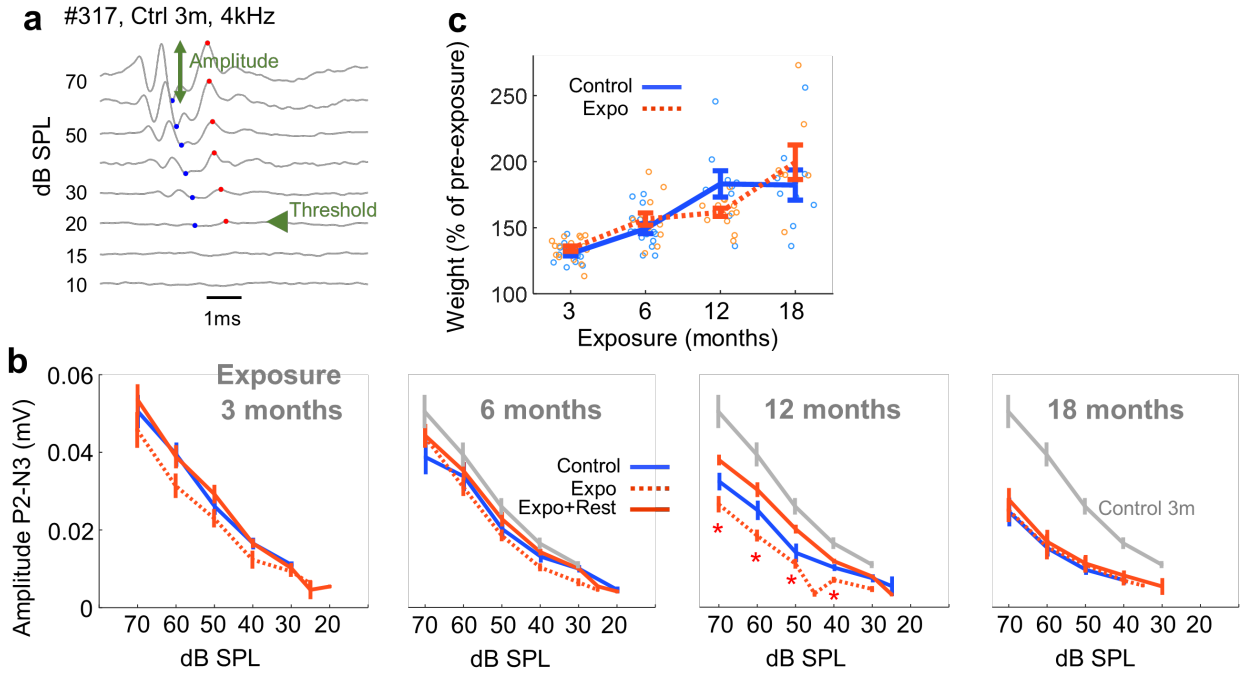

Supp. Fig. 2: a *Individual example of auditory brainstem recordings (ABRs) from which the peak-to-peak amplitude of the largest waves (P2-N3) and the auditory threshold were extracted.* ***b*** *Average P2-N3 amplitude for exposure durations of between 3 (left) and 18 (right) months. Exposure had no significant permanent effect on amplitudes ($F_{3,277}$=0.63, p=0.59). However, there was a significant temporary threshold shift after 3 and 12 months of exposure (Expo vs. Expo+rest, exposure factor, 3 months, $F_{1,93}$=6.65, p=0.01, 6 months, $F_{1,102}$=3.82, p=0.05, 12 months, $F_{1,81}$=68.7, p<1e-10) but not after 18 months ($F_{1,56}$=0.45, p=0.50, t-tests *p<0.05).* ***c*** *Follow-up of the weight of animals in the 18-month exposure group, as a percentage of pre-exposure weight and as a function of exposure duration. Weights obtained after 3, 6 and 12 months of exposure do not include a 3-week rest period. The global difference between exposed and control animals was significant (exposure factor, $F_{1,91}$=21.6, p<1e-10), but there was no individual difference between our animals in post-hoc tests applied to each duration of exposure.*

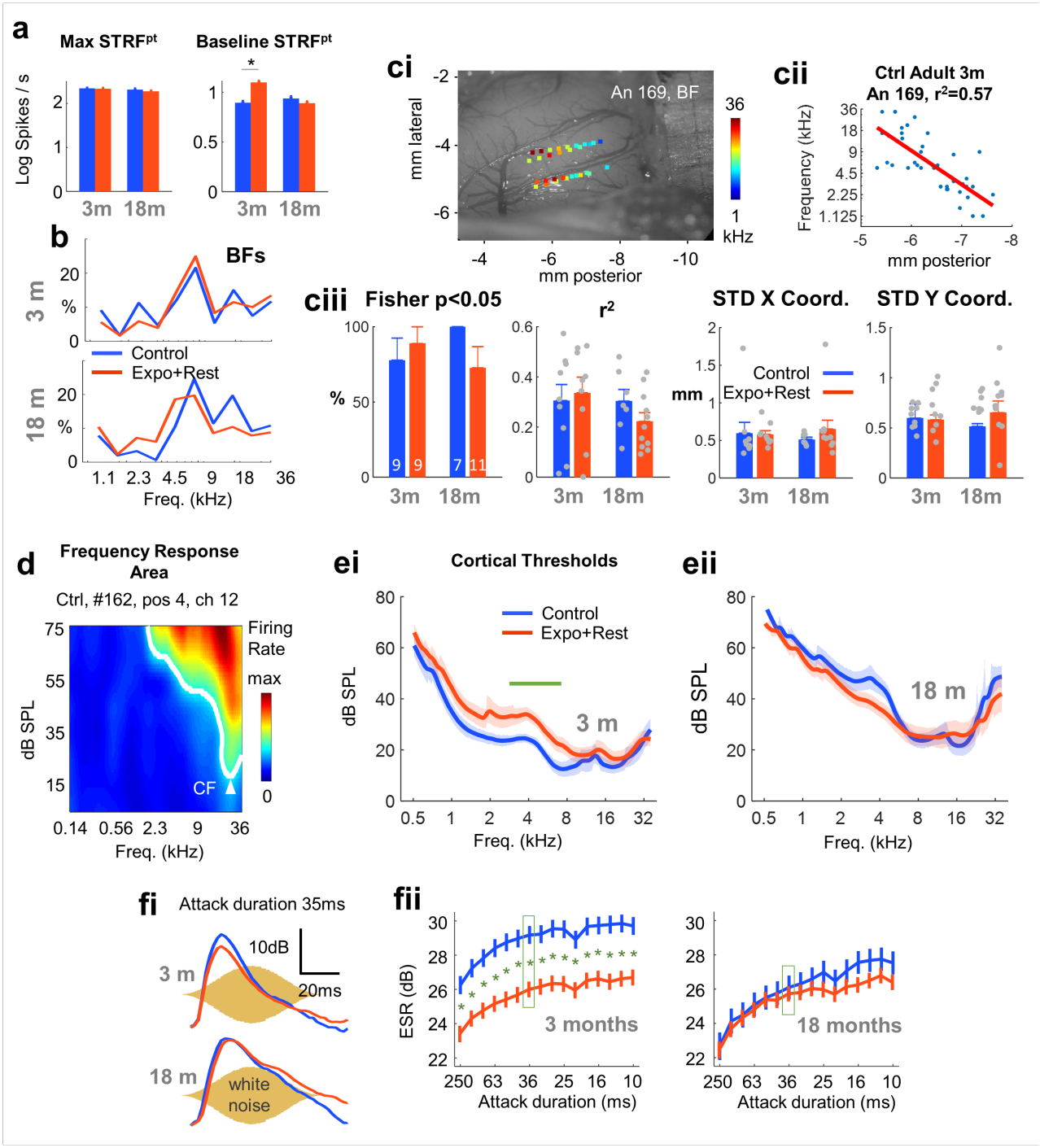

Supp. Fig. 3: a *During quantification of the spectrotemporal receptive fields (STRFs^{pt}), the maximum firing rate remained stable at 75 dB SPL after three months of exposure (left, $F_{1,1625}$=2.33, p=0.13) whereas the baseline firing rate increased (right, $F_{1,1625}$=54.3, p<1e-10; t-tests *p<0.05), like the spontaneous firing rate shown in Fig. 3aiii.* ***b*** *Distribution of best frequency sampling in experimental groups.* ***ci*** *Example of two microarray implantations in the auditory cortex for an exposed animal: the best frequency is color-coded and superimposed on the picture of the auditory cortex for this animal.* ***cii*** *Best frequency of cortical sites implanted in the same animal as a function of anteroposterior distance to bregma. The red line is the linear regression. The topographical organization of best frequencies, i.e. the tonotopy, is clearly visible on this example.* ***ciii*** *Fisher (extreme left) and r^2 (left) statistics extracted from a linear regression of best frequency against antero-posterior coordinates. Standard deviation of anteroposterior coordinates (STD X, right) and mediolateral coordinates for each animal (STD Y, extreme right). Most animals showed a topographical organization of best frequency along the anteroposterior axis as expected (Fisher's test statistically significant) and there was no effect of exposure on r^2, i.e. on the linear fitting of best*

*frequency to the anteroposterior coordinate ($F_{1,32}$=1.1, p=0.3). This result was not dependent on spatial sampling differences, as BF distribution was approximately similar between groups (see **b**) and the dispersion of coordinates was similar between groups (STD X, ANOVA on the four groups, $F_{3,32}$=0.74, p=0.54; STD Y, $F_{3,32}$=0.28, p=0.84). **d** Frequency response area (FRA) of a cortical site in response to tones of various frequencies (abscissa) and intensities in dB SPL (ordinate). The white line is the contour at 6 standard deviations above the spontaneous activity. The characteristic frequency (CF) of the cortical site is defined as the frequency at the minimum intensity required to evoke a significant response. **ei** Average threshold values (evoked discharges 6 standard deviations above spontaneous activity) from the FRA (see **d**) after three months of exposure. **eii** as for **ei** but after 18 months of exposure. Exposure affects cortical thresholds after 3 months, but not 18 months of exposure (factor aging x exposure $F_{1,7842}$=387 p<1e-10, t-tests: the green line indicates the values for which p<0.05 for each frequency). **fi** Average response of all cortical sites to a burst of white noise with a 35 ms rising slope. A decrease in the maximum response is visible after three months of exposure but not after 18 months of exposure. **fii** Quantification of normalized neural response for various rising slope durations (the green rectangle corresponds to the individual example shown in fi). Results obtained after 3 months (top) or 18 months (bottom) of exposure are shown. Exposure for three months led to a decrease in the maximum ESR, whereas exposure for 18 months did not. This was the case whatever the slope of the stimulus rising time ($F_{1,14847}$=85.7, p<1e-10, t-tests in Supp. Fig. 3fii).*

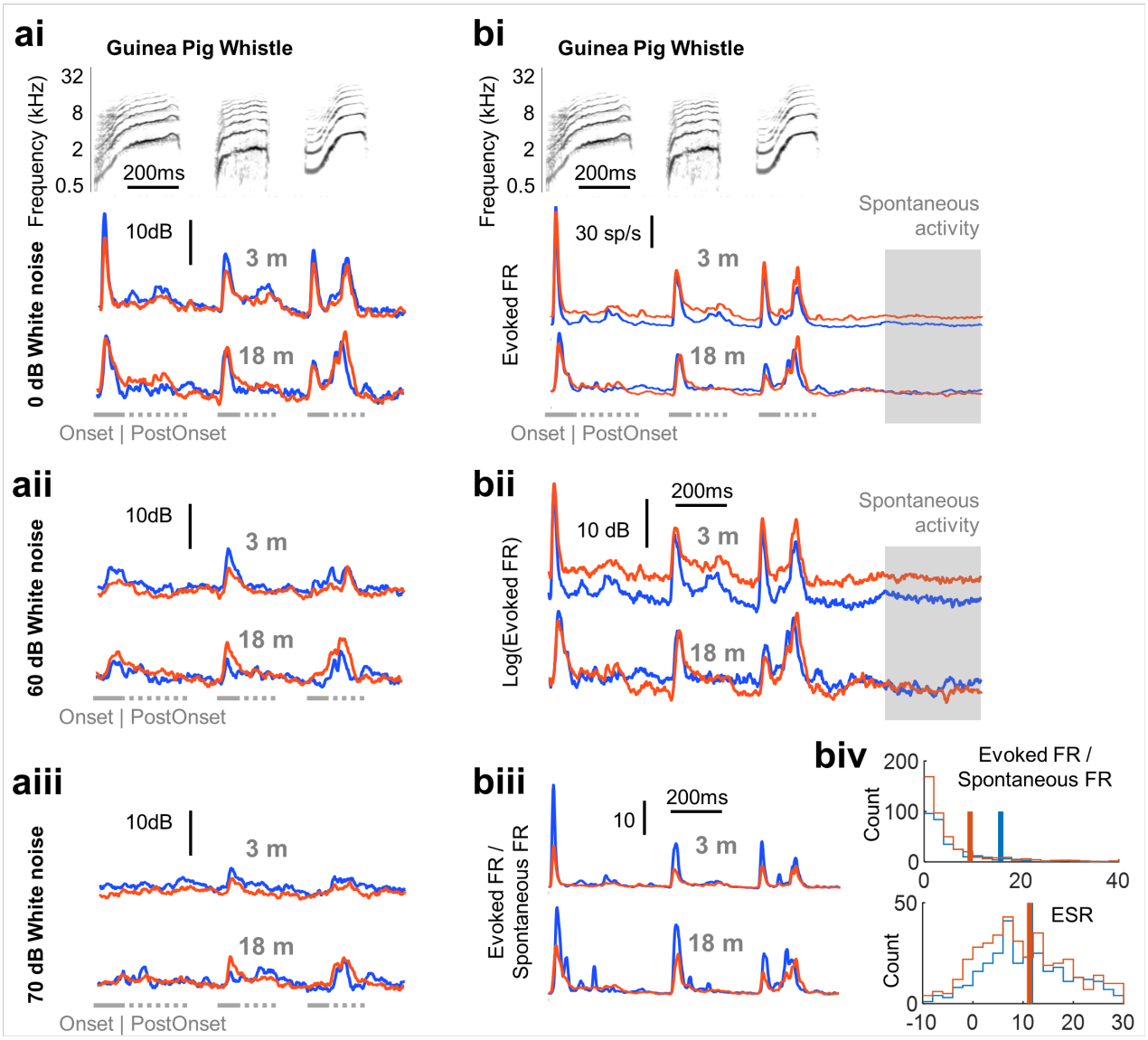

1281

1282 ***Supp. Fig. 3[bis]: ai*** *Same plot as Fig. 3bi: Average response of all cortical sites from each group to three guinea pig*
1283 *whistles (represented by the spectrograms at the top).* ***aii*** *Same as ai with guinea pig whistles presented in 60 dB*
1284 *white noise.* ***aiii*** *Same as ai with guinea pig whistles presented in 70 dB white noise.* ***b*** *Rationale for normalizing*
1285 *and log-transofmring the evoked firing rate* ***bi*** *Average raw evoked firing rate of cortical sites to three guinea pig*
1286 *whistles (represented by the spectrograms at the top). In this protocol, the spontaneous activity is computed by the*
1287 *average of evoked firing rate over the time interval [1300-1750]ms (gray area). There is a clear difference between*
1288 *red and blue curves for the 3-month group which seems to stem from a difference in spontaneous activity similar*
1289 *to that observed in Fig. 3c and Supp. Fig. 3a. This difference confuses the interpretation of differences in evoked*
1290 *firing rate.* ***bii*** *Average Log transform of the evoked firing rate of cortical sites to three guinea pig whistles. The use*
1291 *of a Log transform more clearly emphasizes the problem raised in gi and suggests that a substraction of the Log of*
1292 *average spontaneous activity (i.e. a division of evoked firing rate by the average spontaneous firing rate) would be*
1293 *helpful and pertinent.* ***biii*** *Ratio of evoked firing rate to the average spontaneous firing rate. The baseline shift*
1294 *disappeared compared to* ***bi****. Amplitude of red peaks appears much lower than that of blue peaks. However, this is*
1295 *not the case for the 18-month group when log-transforming the same data as in Fig. 3bi.* ***biv*** *Distribution of the*
1296 *above ratio (upper panel) and of the ESR (lower panel) i.e. log-transform of the ratio, at first peak (latency 34ms).*
1297 *The amplitude difference in peaks in* ***bi*** *occurs because the distribution of peak firing rates for the control group*
1298 *(upper panel) is so skewed that the computation of the average is biased by extreme high values whereas the ESR*
1299 *average is actually similar between the control and the exposed groups.*

1300

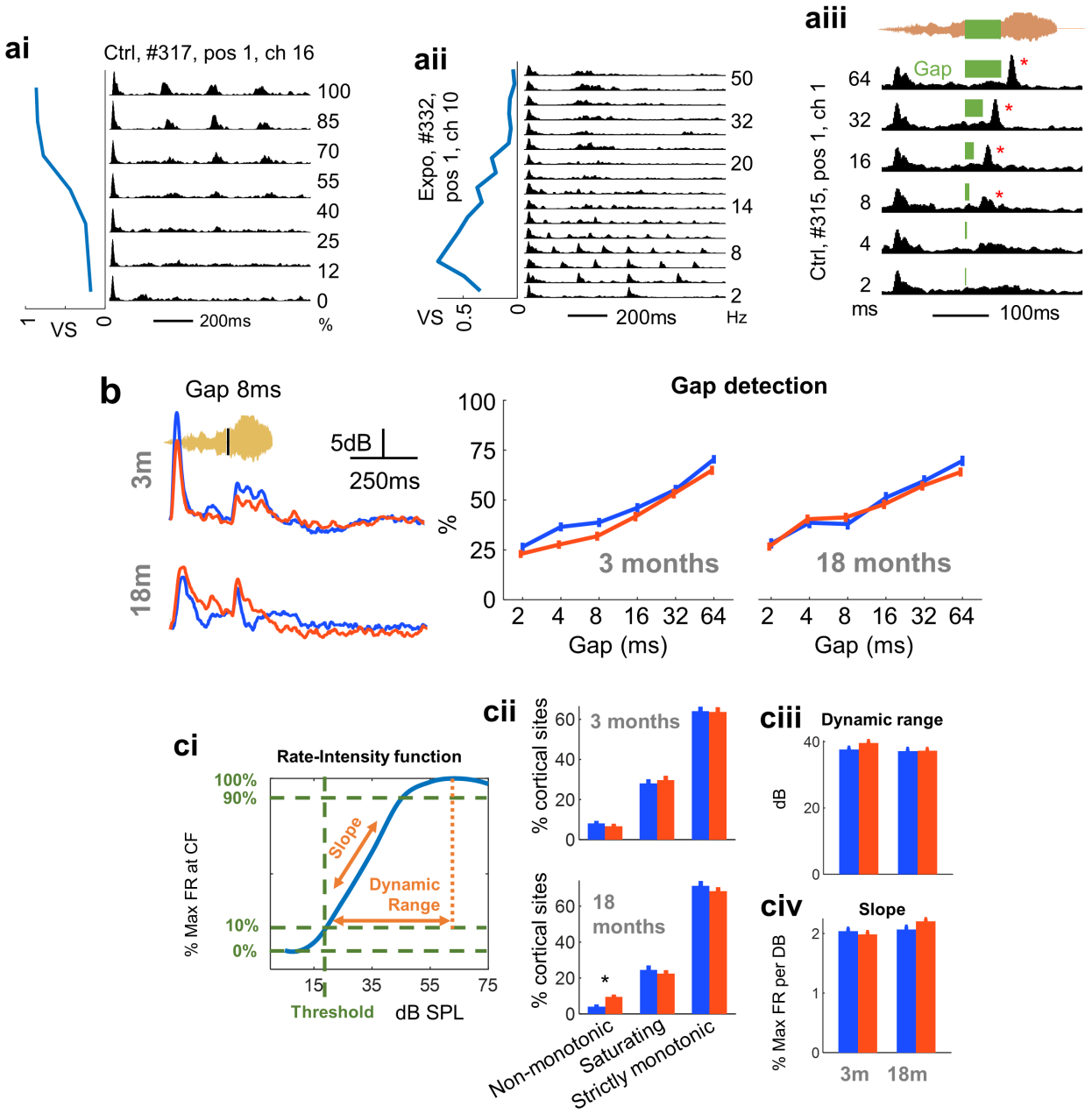

1301

1302 ***Supp. Fig. 4: ai*** *Example of cortical responses to amplitude-modulated white noise with a modulation rate of 4 Hz*
1303 *and a range of modulation depths between 0 and 100%. On the left of the peri-stimulus time histograms (PSTH)*
1304 *for neuronal responses, the depth modulation transfer function is quantified by vector strength (VS, abscissa)*
1305 *plotted as a function of modulation depth.* ***aii*** *As for* ***ai*** *for the responses to a range of modulation rates between 2*
1306 *Hz and 50 Hz at a 100% modulation depth, giving rise to the temporal modulation transfer function in blue.* ***aiii***
1307 *Example of PSTHs for the responses to a guinea pig whistle including gaps of 2-64 ms in duration. The temporal*
1308 *envelope of the guinea pig whistle is represented at the top, with a gap symbolized by a green rectangle. A red star*
1309 *indicates a significant peak in the PSTH within the 50 ms following the gap.* ***b*** *(left) Average response of all cortical*
1310 *sites to a guinea pig whistle including a short (8 ms) gap. (right) Percentage of neurons for which the gap produced*
1311 *a detectable peak in neural response. We were unable to identify a gap duration eliciting a significant difference*
1312 *between animals exposed to noise for 18 months and unexposed animals in terms of the percentage of neurons*
1313 *detecting the gap ($F_{1,9755}$=4, p=4.7e-2, but no significant t-test). The temporal processing of gaps was not, therefore,*
1314 *altered by noise exposure.* ***ci*** *Using the responses at the CF (see Supp. Fig. 3d), we extracted the firing rate-intensity*
1315 *function.* ***cii*** *Classification of rate-intensity function patterns between strictly monotonic, saturating (reaching 90%*
1316 *of the maximum firing rate before 55 dB SPL) and non-monotonic. The percentage of non-monotonic patterns is*

*significantly higher after lifetime noise exposure (proportion test, *p<0.05).* ***ciii*** *Dynamic range and* ***civ*** *slope parameters extracted from the rate-intensity function (see ci). Exposure had no significant effect on dynamic range ($F_{1,1625}$=1.7, p=0.19). The ANOVA test was significant for slope ($F_{1,1625}$=3.91, p=0.048), but none of the pairwise comparisons were significant (p>0.056).*

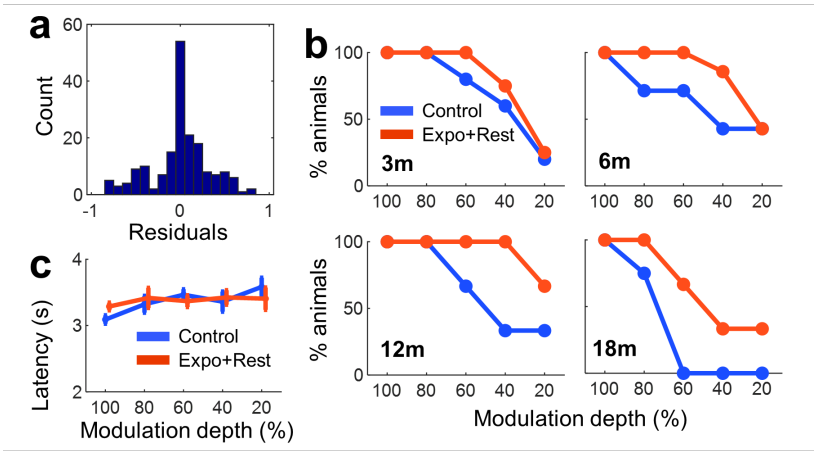

Supp. Fig. 6: Behavioral performance for animals able to learn the task. a *Residuals for the three-way ANOVA model of Fig. 5d. A Jarque-Berra test for normality was performed and it was not possible to reject the null hypothesis (Stat=2.71, p=0.2).* ***b*** *For each exposure duration, the percentage of animals achieving correct discrimination is shown for each modulation depth. Exposure had a positive effect on the discrimination performance of animals, whatever its duration, but the sampling was too limited to draw firm conclusions for each exposure duration.* ***c*** *Mean time lag to change of compartment on CS+ presentation for each modulation depth. Exposure had no effect on this time lag (exposure effect, $F_{1,616}$=0, p=0.97; interaction exposure x duration of exposure, $F_{3,616}$=1.8, p=0.14; interaction exposure x modulation depth, $F_{4,616}$=0.86, p=0.49).*

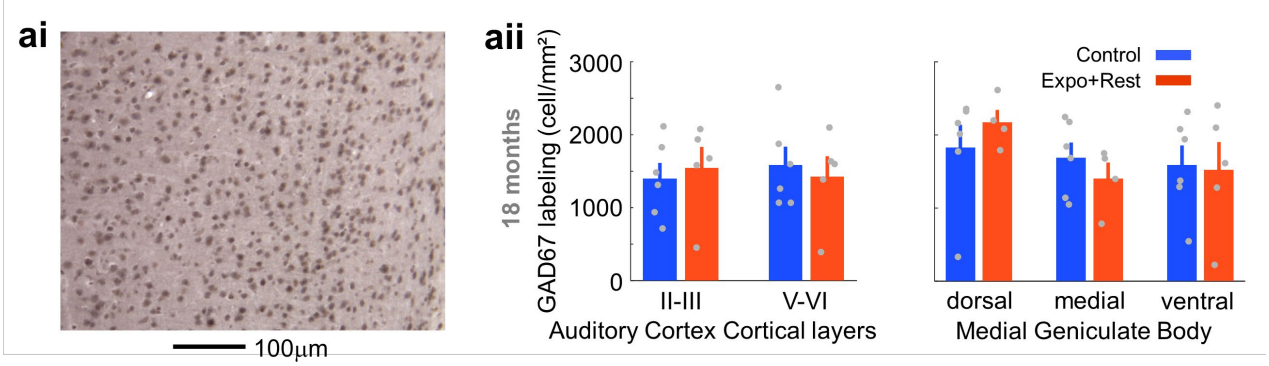

1331

1332 ***Supp. Fig. 7: ai*** *Example of immunostaining for GAD67 in the primary auditory cortex (20 x magnification) of an*
1333 *unexposed animal from the 18-month exposure group.* ***aii*** *Density of GAD67-positive cells in the deep and superficial*
1334 *layers of the auditory cortex (left) and in three divisions of the auditory thalamus, the medial geniculate body (right).*
1335 *Density is compared between exposed and unexposed animals from the 18-month group. Exposure had no*
1336 *significant effect in the auditory cortex ($F_{1,18}$=0.37, p=0.55) or the auditory thalamus ($F_{2,25}$=0.61, p=0.55).*

1337